TECHNISCHE UNIVERSITÄT WIEN
Vienna University of Technology

DIPLOMARBEIT

# Design of a user-controllable system for self-assembly of multiple DNA origami platforms on a 2D surface

zur Erlangung des akademischen Grades

**Diplom-Ingenieurin**

Im Rahmen des Studiums

**Biomedical Engineering**

eingereicht von

**Caroline May Hammoutene**

Matrikelnummer 00927127

ausgeführt am Institut für Angewandte Physik,
Fakultät für Physik Technischen Universität Wien

**Betreuung**
Univ.Ass Dipl.-Ing. Dr.techn Joschka Hellmeier BSc
Ass. Prof. Dipl.-Ing. Dr. Eva Sevcsik

Die approbierte gedruckte Originalversion dieser Diplomarbeit ist an der TU Wien Bibliothek verfügbar
The approved original version of this thesis is available in print at TU Wien Bibliothek.
TU WIEN Bibliothek Your knowledge hub

Die approbierte gedruckte Originalversion dieser Diplomarbeit ist an der TU Wien Bibliothek verfügbar
The approved original version of this thesis is available in print at TU Wien Bibliothek.

1.

Diese Arbeit ist jenen gewidmet die mich im Laufe der Jahre unterstützt haben.

DANKE.

Ce travail est dédié à tous ceux qui m'ont soutenu au fil des années.

MERCI.

| | | |
|---|---|---|
| Mutti | Papa | Claire |
| Großvater | Udl | Tara |
| Doris | Jakob | Laura |
| Raphi | Stefan | Joschka & Eva |

Die approbierte gedruckte Originalversion dieser Diplomarbeit ist an der TU Wien Bibliothek verfügbar
The approved original version of this thesis is available in print at TU Wien Bibliothek.
TU WIEN Bibliothek Your knowledge hub

# Kurzzusammenfassung

DNA-Origami, ein Gebiet innerhalb der DNA-Nanotechnologie und die Methode, die in dieser Master-Arbeit verwendet wurde, ist ein sehr vielversprechender Weg, um DNA als Material zu verwenden. Das Ziel dieser Arbeit war es, rechteckige DNA-Origami-Plattformen mit einem Seitenverhältnis von 2:1 herzustellen. Weiters sollte das Zusammenfügen von DNA Origami Plattformen zu größeren Strukturen durch Zugabe definierter Interaktions-DNA-Strängen möglich sein.

Nach dem computergestützten Design der Plattform mit caDNAno und der Analyse der Effizienz des DNA-Strangeinbaus mit canDo wurden die nötigen DNA Stränge bestellt und die DNA-Origami-Plattformen nach einem Faltungsprotokoll gefaltet. Zur Charakterisierung wurden verschiedene Methoden verwendet: Gelelektrophorese zur Größenbestimmung, Konzentrationsmessungen zur Detektion der Faltungsausbeute und Rasterkraftmikroskopie zur Visualisierung der richtigen Faltung.

Die DNA-Origami-Plattformen wurden über Cholesterin-Einheiten auf einer Lipid-Doppelschicht verankert und unter Verwendung von Einzelmolekül-Fluoreszenzmikroskopie sichtbar gemacht. Bindungsstränge wurden zugegeben um frei diffundierende Rechtecke miteinander zu verbinden. Einzelmolekül-Fluoreszenzmikroskopie wurde verwendet, um die Aggregation von DNA-Origami-Plattformen zu größeren Strukturten zu beobachten. Eine teilweise Ablösung der Aggregate von der Lipiddoppelschicht sowie sehr große Konglomerate wurden beobachtet. Dies deutet darauf hin, dass die Wahl der Anzahl der Interaktionsstellen zwischen DNA-Origami-Plattformen sowie zwischen einer DNA-Origami-Plattform und der Lipid-Doppelschicht entscheidend für ein erfolgreiches Experiment ist. Alternativen zur Verankerung von DNA-Rechtecken über Cholesterin-Einheiten an einer Lipiddoppelschicht zu Oligomerisierungszwecken sollten in Betracht gezogen werden.

Die approbierte gedruckte Originalversion dieser Diplomarbeit ist an der TU Wien Bibliothek verfügbar
The approved original version of this thesis is available in print at TU Wien Bibliothek.
TU WIEN Bibliothek Your knowledge hub

# Abstract

DNA origami, a field within DNA nanotechnology and the method used for the work done in the scope of this thesis, is a very promising way of using DNA as a material. The goal of this work was to create rectangular scaffolded DNA origami platforms with an aspect ratio 2:1 that allow predefined positioning of interaction strands to initiate self-assembly into larger structures.

After computationally designing the platform with caDNAno, and analyzing the strand incorporation efficiency using canDo, the DNA origami platforms were produced following a folding protocol. For the purpose of their characterization, different methods were uses: gel electrophoresis for size estimation, concentration measurements for determining the folding yield and atomic force microscopy for visualization of proper folding.

The DNA origami platforms were anchored to a lipid bilayer via cholesterol moieties and imaged using single molecule fluorescence microscopy. Binding strands were added so that freely diffusing platforms bind to each other. Single molecule fluorescence microscopy was used to observe aggregation of DNA origami platforms to larger assemblies. Partial detachment of the aggregates from the lipid bilayer as well as formation of very large conglomerates was observed. This indicates that the choice of number of interaction sites between DNA origami platforms as well as between a DNA origami platform and the lipid bilayer is crucial for a successful experiment. Alternatives to anchoring DNA rectangles via cholesterol moieties to a lipid bilayer for oligomerization purposes should be taken under consideration.

Die approbierte gedruckte Originalversion dieser Diplomarbeit ist an der TU Wien Bibliothek verfügbar
The approved original version of this thesis is available in print at TU Wien Bibliothek.
TU Bibliothek Your knowledge hub WIEN

# Eidesstattliche Erklärung

Ich erkläre an Eides statt, dass ich die vorliegende Arbeit selbstständig verfasst, andere als die angegebenen Quellen/Hilfsmittel nicht benutzt, und die den benutzten Quellen wörtlich und inhaltlich entnommenen Stellen als solche kenntlich gemacht habe. Das in TISS der TU Wien hochgeladene Textdokument ist mit der vorliegenden Dissertation ident.

Wien, 09.10.2021

Ort, Datum

Unterschrift

Die approbierte gedruckte Originalversion dieser Diplomarbeit ist an der TU Wien Bibliothek verfügbar
The approved original version of this thesis is available in print at TU Wien Bibliothek.
TU Bibliothek Your knowledge hub WIEN

Die approbierte gedruckte Originalversion dieser Diplomarbeit ist an der TU Wien Bibliothek verfügbar
The approved original version of this thesis is available in print at TU Wien Bibliothek.

# Table of Contents

**Kurzzusammenfassung** ..... i

**Abstract** ..... ii

**Eidesstattliche Erklärung** ..... iii

**1 Background** ..... 1

1.1 DNA Nanotechnology ..... 2

1.1.1 Structure and Properties of DNA ..... 2

1.1.2 DNA Nanotechnology ..... 4

1.1.3 DNA Origami ..... 6

1.1.4 Supported Lipid Bilayer ..... 10

1.2 Microscopy ..... 13

1.2.1 Fluorescence Microscopy ..... 13

1.2.2 Atomic Force Microscopy ..... 20

**2 Introduction** ..... 23

2.1 Project rationale ..... 23

2.2 Approach and Experimental Setup ..... 25

**3 Material and Methods** ..... 28

3.1 Computational design of the DNA Origami ..... 28

3.2 Preparation of DNA Origami ..... 28

3.2.1 DNA origami folding buffer conditions ..... 29

3.2.2 Folding of DNA origami and addition of binding strands ..... 29

..... 31

3.2.3 Spin Column Purification ..... 31

3.3 Quality control and characterization of DNA Origami ..... 32

3.3.1 Gel Electrophoresis ..... 32

3.3.2 Concentration measurement with NanoDrop ..... 33



Die approbierte gedruckte Originalversion dieser Diplomarbeit ist an der TU Wien Bibliothek verfügbar
The approved original version of this thesis is available in print at TU Wien Bibliothek.
TU Bibliothek Your knowledge hub WIEN

3.3.3 Atomic Force Microscopy ..... 33

3.4 Supported Lipid Bilayer Production ..... 34

3.4.1 Production of lipid vesicles ..... 34

3.4.2 Production of supported lipid bilayer ..... 35

3.4.3 Addition of DNA-cholesterol anchors ..... 35

3.4.4 Labeling and addition DNA origami ..... 35

3.5 Total Internal Reflection Fluorescence Microscopy ..... 36

3.5.1 Diffusion Coefficient ..... 36

3.5.2 Oligomerization ..... 36

**4 Results and Discussion ..... 37**

4.1 Computational design of DNA origami rectangles ..... 37

4.2 Characterization of DNA origami rectangles ..... 42

4.2.1 Gel Electrophoresis ..... 43

4.2.2 Determination of yield ..... 45

4.2.3 AFM ..... 45

4.2.4 TIRF microscopy ..... 46

**5 Conclusion and Outlook ..... 51**

**6 Appendix ..... 52**

6.1 Abbreviations ..... 52

6.2 List of sequences ..... 53

**List of Figures ..... 58**

**List of Tables ..... 59**

**Bibliography ..... 60**

Die approbierte gedruckte Originalversion dieser Diplomarbeit ist an der TU Wien Bibliothek verfügbar
The approved original version of this thesis is available in print at TU Wien Bibliothek.
TU WIEN Bibliothek Your knowledge hub

Die approbierte gedruckte Originalversion dieser Diplomarbeit ist an der TU Wien Bibliothek verfügbar
The approved original version of this thesis is available in print at TU Wien Bibliothek.

# 1 Background

"DNA in a material world" [1] , is the title of an article written by Nadrian C. Seeman, who is considered to be the founder of DNA nanotechnology. Deoxyribonucleic acid (DNA), is most commonly known as the carrier of the genetic information in all living cells. By publishing his work on the formation of junctions and lattices out of nucleic acids [2] in 1982, Seeman revolutionized the way science looks at DNA and created a paradigm shift towards using DNA as a material.

With the invention of the "scaffolded DNA origami" [3] method, by Paul Rothemund, first published in his article "Folding DNA to create nanoscale shapes and patterns" in 2006, the world of nanotechnology has again been revolutionized.

Today, four decades later, DNA nanotechnology is a promising field of research and of commercial interest [4] because of its ability to create nanoscopic scale sized structures. Let alone in the last decade its broad range of emerging applications such as targeted drug delivery [5]–[8] for personalized medicine, nanoscale sensors [9], [10] and robotic arms [11], [12] emphasize the significance of DNA nanotechnology and DNA based nanodevices [13].

In this work I will analyze the assembly behavior of rectangular DNA origami platforms and their possible formation of oligomers considering different locations of incorporated binding sites on the edges of the DNA origami. For a better understanding I will first give some background information and give an introduction. I will further describe the materials and the methods used, show the results and discuss them.

The aim of the work done for this thesis, is to make a small contribution to the ongoing research in the field of DNA nanotechnology and specifically to the project to form "target delivery units from rectangular patchy particles" described in a following section.

Die approbierte gedruckte Originalversion dieser Diplomarbeit ist an der TU Wien Bibliothek verfügbar
The approved original version of this thesis is available in print at TU Wien Bibliothek.
TU WIEN Bibliothek Your knowledge hub

## 1.1 DNA Nanotechnology

### 1.1.1 Structure and Properties of DNA

DNA, is short for deoxyribonucleic acid, a macromolecule found in all living organisms. It is the carrier of genetic information, coding instructions for protein synthesis. There are three major forms of DNA, A-form, B-form and Z-form DNA. In the following DNA always refers to the B-form DNA. DNA consists of three types of chemical components forming nucleotides: deoxyribose, a sugar, a phosphate and four nitrogenous bases. These bases are adenine (A), guanine (G), cytosine (C) and thymine (T). Whereas cytosine and thymine each have a single-ring structure called pyrimidine, adenine and guanine each have a double-ring structure called purine. These four possible nucleotides are the fundamental building blocks of DNA.

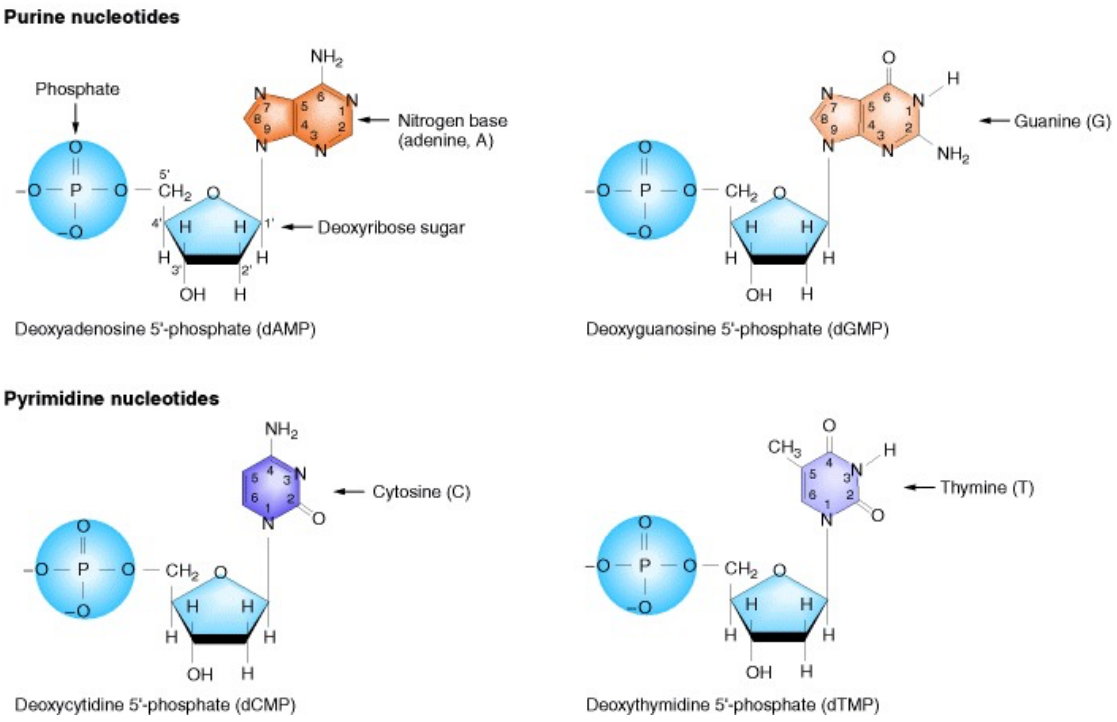


*Figure 1 Chemical Structure of the four Nucleotides*

*Schematic sketches of purine and pyrimidine nucleotides each composed of a phosphate group, a sugar and a nitrogen base, Adenine, Guanine, Cytosine or Thymine. Image taken form [14]*

Due to phosphodiester bonds, bonds between the sugar and the phosphate, representing the backbone of DNA strands, nucleotides form chains. DNA consists of two strands twisted into the structure of the double helix. Within this double helix, holding the two strands together, the



Die approbierte gedruckte Originalversion dieser Diplomarbeit ist an der TU Wien Bibliothek verfügbar
The approved original version of this thesis is available in print at TU Wien Bibliothek.
TU Bibliothek Your knowledge hub WIEN

nitrogenous bases form bonds in a specific manner discovered by and named after James Watson and Francis Crick, the Watson-Crick base pairing rules [15]. Guanine only binds with cytosine by formation of three hydrogen bonds and thymine only binds with adenine by formation of two hydrogen bonds. These bases binding with each other are called complementary bases. The base pairs are flat planar structures *(Figure 2 (e)).*

These structures undergo basestacking which contributes to the stability of a DNA molecule. Basestacking is responsible for the formation of a major and minor groove within the DNA double helix.

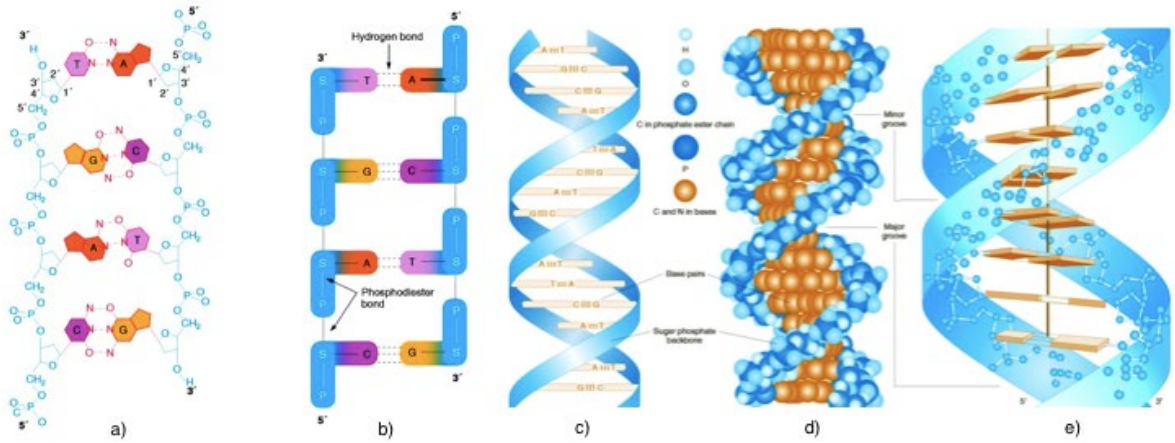


***Figure 2 Five representations of the DNA Double Helix***

*a) shows an unwind chemical diagram of the DNA double helix, with its sugar-phosphate backbone colored in blue and its bases connected via hydrogen bonds in the middle of the molecule. b) is a simplified representation emphasizing on the antiparallel structure. c) is a simple representation of the DNA double helix ladder, d) depicts the density of its molecular structure as space filling model and e) emphasizes on the base pair arrangements responsible for base stacking and major and minor groove formation. Images were adapted form [14]*

A phosphodiester bond is between the phosphate and the 5’ carbon of the deoxyribose on the one side and between the phosphate and the 3’ carbon on the other side (*Figure 2 (a))*. The double-stranded DNA molecule has its backbones organized in an antiparallel manner, one strand oriented from 5’ to 3’ and the other form 3’ to 5’. As mentioned above guanine and cytosine base pairs are bound by three hydrogen bonds, one more than adenine and thymine. The more guanine and cytosine base pairs a DNA double helix contains the more stable it is, meaning that the separation of two strands, called denaturation or melting, is less likely than with a DNA double helix composed of more adenine and thymine base pairs. Therefore, the higher the guanine-cytosine content the higher the melting point temperature. But by only using G-C combinations, complex secondary structures would occur, which would make practical application extremely difficult.

Die approbierte gedruckte Originalversion dieser Diplomarbeit ist an der TU Wien Bibliothek verfügbar
The approved original version of this thesis is available in print at TU Wien Bibliothek.
TU Bibliothek Your knowledge hub WIEN

### 1.1.2 DNA Nanotechnology

DNA nanotechnology uses DNA as a building material to create objects of different shapes and sizes on the nanoscale to the microscale with high spatial resolution < 10 nm [16]. The advantage of using DNA as a material is that besides its biocompatibility out of all natural or synthetic molecules it has the most programmable and predictable interactions [7]. Due to the specific binding properties of DNA, its thermodynamic stability, the rapid synthetization possibilities [17] and many options to further tune and modify the structure of DNA such as by using DNA-acting enzymes [18] or by facilitating interactions between DNA origami structures [19], DNA represents a remarkable building material. The fields of applications envisioned for DNA nanotechnology are broad such as nanofabrication and medicine [7]. In the following I will give an overview of the wide range of achieved advancements in the field of DNA nanotechnology.

The first approach of working with DNA as a material has been undertaken by Ned Seeman in the 1980s when he first realized connecting six-arm branched junctions together using Watson-Crick base pairing of the sticky ends, the single stranded overhangs, to form 3D crystalline structures [2]. Little less than a decade later the construction of a closed cube out of DNA has been reported [20]. In 1998 the self-assembly into 2D crystalline forms has been designed and observed by atomic force microscopy [21] and a year later dynamic assemblies such as switchable molecular machines have been realized [22]. Six years later, the formation of triangles out of flexible DNA four-arm junctions [23] and the invention of a DNA built walking motor [24] were reported. Further RNA nanotechnology has been introduced in the same year. In 2006 presumably nowadays the most famous method in the field of DNA nanotechnology has been published by Paul Rothemund: DNA origami [3] which is a method that uses one long and many short synthetic DNA strands that fold into a wanted two- or three-dimensional shape. Then for example box with a controllable lid [25], an autonomous walking device out of DNA [26] or a responsive nanorobot for targeted delivery [27] have been realized. In 2012, another method within DNA nanotechnology was invented by Bryan Wei and his team: DNA bricks [28]. Opposed to DNA origami, DNA bricks only use short synthetic DNA strands that interlock into bricks, like Legos, into the wanted two- or three-dimensional shape. Amongst other things DNA was used for visualization of biological events by using high speed atomic

Die approbierte gedruckte Originalversion dieser Diplomarbeit ist an der TU Wien Bibliothek verfügbar
The approved original version of this thesis is available in print at TU Wien Bibliothek.
TU Bibliothek Your knowledge hub WIEN

force microscopy [29], to form hybrid structures out of proteins and DNA [30] and the stability of DNA structures under challenging experimental conditions [31] in the years that followed.

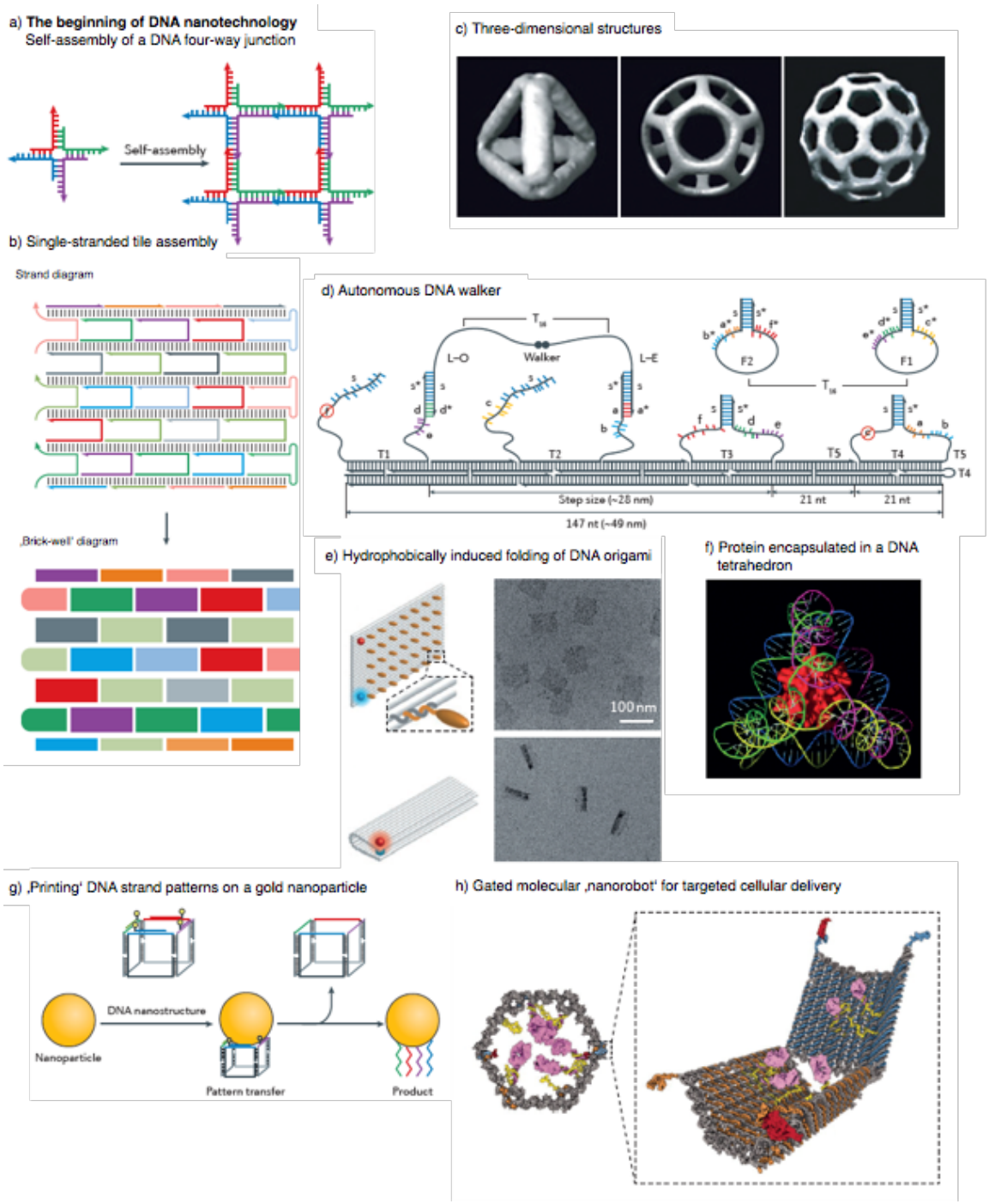


*Figure 3 DNA nanotechnology*

*a) The beginning of DNA nanotechnology: DNA four-way junction, self assembles into a square shape.[7] b) Visualization of the single stranded tile assembly showing a strand diagram and a "Brick-wall" diagram [28] c) Three dimensional structures form DNA: DNA crossover tile assembly [32] d) Dynamic DNA nanostructures: autonomous DNA walker [26] e) self-folding*



Die approbierte gedruckte Originalversion dieser Diplomarbeit ist an der TU Wien Bibliothek verfügbar
The approved original version of this thesis is available in print at TU Wien Bibliothek.
TU Bibliothek Your knowledge hub WIEN

*DNA origami rectangle due to interacts with cholesterol [33] f) Protein encapsulation using a DNA tetrahedron [34] g) Nanoparticle assembly with DNA [35] h) Biological application of DNA nanotechnology: Cage with encapsulated antibody [27]*

As the number of patent applications and publications in the field of DNA nanotechnology is gradually increasing the rise of more entrepreneurial activity is expected which maybe leading to a wide ranged commercialization of DNA nanotechnologies [4].

In the following section I will, in detail, explain probably the most prominent method of using DNA as a material which is also the method used for the work of this thesis: scaffolded DNA origami.

### 1.1.3 DNA Origami

Today, scaffolded DNA origami, the method Paul Rothemund stands for as inventor, is a state-of-the-art tool in the field of DNA nanotechnology.

#### 1.1.3.1 Basic terms and conditions

A viral *scaffold strand* is a long single stranded circular genomic DNA, usually taken from the virus M13mp18 discovered at the Max Planck Institute of Biochemistry [3]. It is a sequence of 7,249 nucleotides used as starting point for folding DNA into a specific shape. *Staple strands* are short single stranded DNA fragments that are designed to complementarily bind the scaffold strand at specific regions, usually consisting of 16 to 50 nucleotides [3]. After the design process, the desired structure comes into shape due to the binding of the staple strands to the scaffold strands. While the scaffold strand is extracted from the virus, the staple strands are chemically synthesized.

By designing the staple strands in a way that they complementarily bind to the scaffold strand in a specific manner, one can determine the way a structure is folded and therefore its stability. This is facilitated by designing *crossovers* that connect one row of the scaffold strand with another. (*Figure 4*).

One complete turn of a DNA double helix is 3.4 nm or 10 base pairs long, the distance between two base pairs is 0.34 nm, and the helical diameter is 2 nm.

Die approbierte gedruckte Originalversion dieser Diplomarbeit ist an der TU Wien Bibliothek verfügbar
The approved original version of this thesis is available in print at TU Wien Bibliothek.
TU Bibliothek Your knowledge hub WIEN

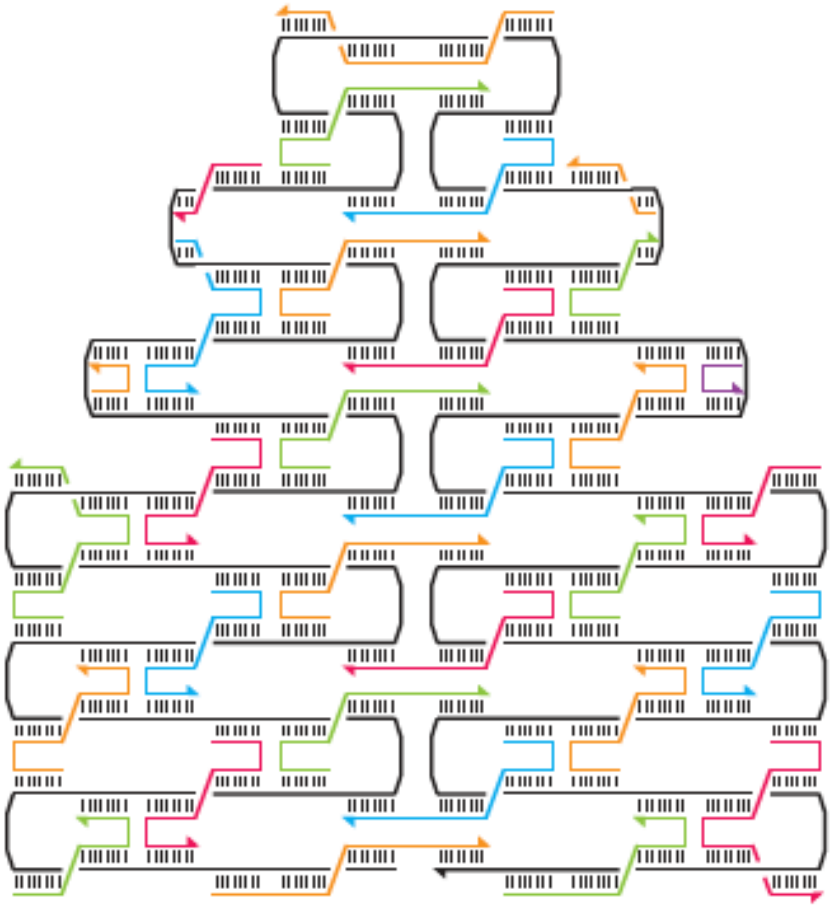

*Figure 4 Schematic drawing of folded DNA origami structure*

*A long black scaffold strand held together by colored staple strands crossing over to adjacent rows folding the scaffold strand into a wanted shape- Image adapted from[3].*

#### 1.1.3.2 Creating a DNA origami platform

By developing the state of the art software caDNAno [36] Shih and his colleges simplified the DNA origami design process of any 2D and 3D object using either a square lattice for 2D and the honey comb lattice for 3D projects. To facilitate the design process within the open source software used for designing a DNA origami structure, 10.5 bases represent one turn which is 3.6nm long. The scaffold strand and the staple strands are arranged in an antiparallel manner along defined rows and columns depending on the wanted shape of the design. Every 16 bases or every off number of half-turns there is a possibility for crossovers, which allow strands to cross over to adjacent rows for further strand placement. This results in an inter-helix gap of 1nm.

To analyze properties such as stress, or incorporation efficiency, the open source web platform CanDo [37], [38] can be used. By calculating the root mean square fluctuation (RMSF) and



Die approbierte gedruckte Originalversion dieser Diplomarbeit ist an der TU Wien Bibliothek verfügbar
The approved original version of this thesis is available in print at TU Wien Bibliothek.
TU Bibliothek Your knowledge hub WIEN

heatmapping the design according to the RMSF values it is possible to deduce the thermal fluctuations and mechanical stress of the DNA origami platform. After the design is finished the staple strands can be ordered or synthesized for DNA origami production. For folding, a specific folding buffer (FoB) is used. The ingredients of such FoB have different properties: Whereas Tris ensures the stability of the pH value of the solution and EDTA chelates cations and inactivates DNase, the addition of NaCl facilitates hydrogen bond formation. $Mg^{2+}$ enables the self-assembly process of the DNA into the desired DNA origami structures. As $Mg^{2+}$ immediately reacts with EDTA, which drastically reduces the quality of the folding buffer, it is only added shortly before usage. A mixture of staple strands, scaffold strand and buffer solution is heated up to 90°C and then cooled down following a defined protocol. Staple strands are typically added in 10-fold excess to augment the probability of strand incorporation. Once the strands in the mixture lose their possibly formed secondary structure and denaturate in the short heat-up phase, they anneal and form the wanted shape in the long cool-down phase observed within the temperature range of 60°C to 40°C [39]. In order to remove excessive strands after the folding process, a purification step, such as spin column purification, is needed which will be explained in detail in the methods section.

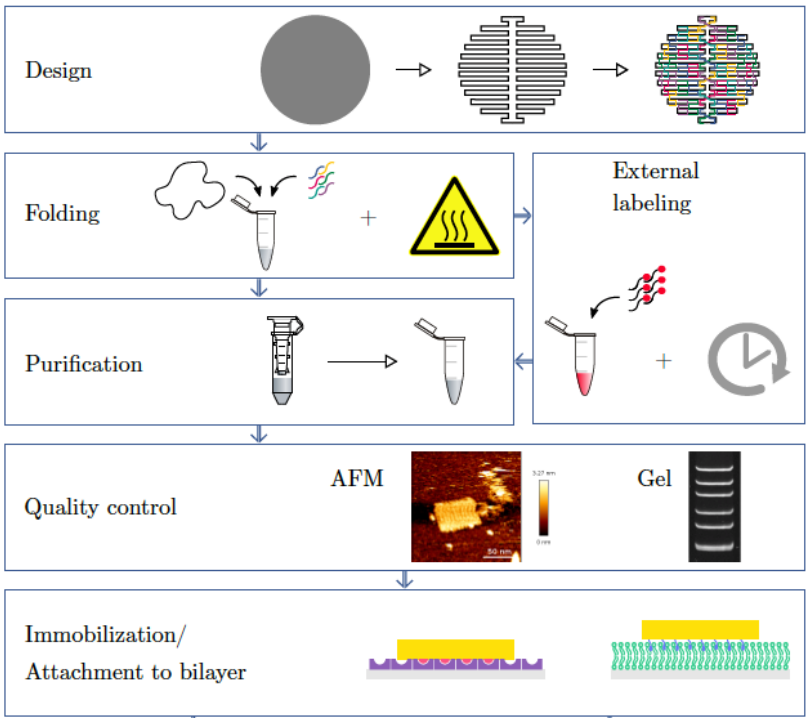


*Figure 5 Workflow DNA origami*

*This flowchart shows the steps to be done to achieve a DNA origami platform and the analysis of such. The working steps done for this thesis are described in the following chapters and sections.[40]*



Die approbierte gedruckte Originalversion dieser Diplomarbeit ist an der TU Wien Bibliothek verfügbar
The approved original version of this thesis is available in print at TU Wien Bibliothek.
TU Bibliothek Your knowledge hub WIEN

#### 1.1.3.3 Self-assembly on 2D surfaces

For the purpose of this work as well as for many applications in the field of DNA origami nanotechnology a large-scale self-assembly process of DNA origami into lattices is necessary. In this section I will introduce ways to bind DNA origami platforms to two different surfaces used in this thesis, mica and a lipid bilayer, and three possible ways to provoke the self-assembly process on these surfaces: close packing, blunt-end stacking interactions and strand hybridization.

For an assembly process the right surface has to be chosen. Depending on the properties wanted the most used surfaces are mica and lipid bilayers. Mica is a mineral that is build up by elastic and flat parallel layer structures with low binding between the layers. This structure enables mica to be cleaved by using duct tape resulting in a nearly perfectly flat strongly negative charged surface. As DNA is a negatively charged polymer, monovalent cations are needed to facilitate electrostatic induced adhesion. Adsorption can be facilitated by adding $Mg^{2+}$ acting as salt bridge between DNA and mica. By adding monovalent ions, e.g. $Na^{+}$, the charge between the mica and the DNA origami gets more diffuse, weakening their interaction, resulting in a higher mobility of the DNA origami on the surface [41].

Another commonly used way to facilitate diffusing DNA origami on a surface is by using a supported lipid bilayer. I will describe its structure and properties in detail in the following section. Other than with mica, in order to adhere DNA origami to a supported lipid bilayer, DNA-modified cholesterol anchors are used to facilitate binding. Cholesterol-DNA strand binds to an elongated staple strand on the DNA origami by complementary base pairing with its DNA end and to the lipid bilayer with its cholesterol moiety, acting as membrane anchors [42] and facilitating diffusion. When the DNA origami structures are placed on a surface where they can diffuse, the self-assembly process can be initiated.

One way to do that is by blunt end stacking. The blunt end of a double stranded DNA molecule refers to the fact that both strands of the DNA end with a base pair. When considering sticky-ends, or overhanging ends, as opposed to blunt-ends, one or both ends of a double-stranded DNA are single-stranded. Blunt-end stacking interactions [19] allows for reversible base attachment and detachment and therefore for reorganization and correction of assembled structures. In this way, blunt ends facilitates bond forming between structures on their borders [19].



Die approbierte gedruckte Originalversion dieser Diplomarbeit ist an der TU Wien Bibliothek verfügbar
The approved original version of this thesis is available in print at TU Wien Bibliothek.
TU Bibliothek Your knowledge hub WIEN

Another way for self-assembly of DNA origami is by using sticky ends [42]. This method provokes stronger irreversible interactions between the DNA origami. When using this method, the sticky ends of two DNA origami are designed to bind to each other through regular base pairing.

An alternative to self-assembly is diffusion-assisted close packing [41]. The principal here is to pack as many structures for example on a mica so that they fill the whole area. The steric repulsion between the DNA origami determines their arrangement.

In this thesis the following method was used: Interaction strands were bound to unpaired areas of the scaffold strand on one end and left unpaired and therefore, hanging over on the other end. Binding strands where then introduced to the system, designed to bind via hybridization to the overhanging ends of the interaction strands on the one side and bind with each other on the other side. One advantage of this method is that the strength of the interaction can be easily controlled by the number and type of base pairs.

### 1.1.4 Supported Lipid Bilayer

Amphipathic lipids have a hydrophobic and a hydrophilic part which is a crucial property needed for lipid bilayer formation. Phospholipids are the most common membrane lipids, having a hydrophilic head group and two hydrophobic tails. These two tails can differ in their length and their structure, one can be saturated and the other unsaturated (has one more cis-double bonds). The quality of a supported lipid bilayer, for example the fluidity of the membrane, varies strongly dependent on the properties of the chains.

In aqueous environments amphipathic lipids spontaneously either form bilayers or micelles depending on the free energy. The hydrophilic parts either form hydrogen bonds or favorable electrostatic interactions with water whereas the hydrophobic tails are insoluble in water and do not interact in a favorable manner. Water that surrounds hydrophobic molecules forms into ice-like cages around them. In order to minimize the energy needed, hydrophobic molecules form cluster. When interaction with each other they immediately bury their hydrophobic parts and form either bilayers of spherical micelles. The same forces are accountable for the self-healing properties of a lipid bilayer. If a small rupture occurs the lipids rearrange so that again only the hydrophilic parts can interact with water and form a sealed compartment, a sphere.

In order to mimic a cell membrane a planar supported lipid bilayer which forms on a solid surface, such as a glass coverslip, is used by taking advantage of the electrostatic properties of



Die approbierte gedruckte Originalversion dieser Diplomarbeit ist an der TU Wien Bibliothek verfügbar
The approved original version of this thesis is available in print at TU Wien Bibliothek.
TU Bibliothek WIEN Your knowledge hub

lipids. Therefore, small unilamellar lipid vesicles (SUVs), were put on a plasma cleaned hydrophilic cover slip. The vesicles are adsorbed to the surface and start fusing with neighboring vesicles getting larger which increases the likelihood of rupture. This is how a planar lipid bilayer starts to form [43]. In order to rupture the remaining vesicles, the partially formed lipid bilayer is washed with a buffer containing a low salt concentration creating osmotic pressure responsible for further ruptures and the complete formation of a planar supported lipid bilayer.

Die approbierte gedruckte Originalversion dieser Diplomarbeit ist an der TU Wien Bibliothek verfügbar
The approved original version of this thesis is available in print at TU Wien Bibliothek.
TU WIEN Bibliothek Your knowledge hub

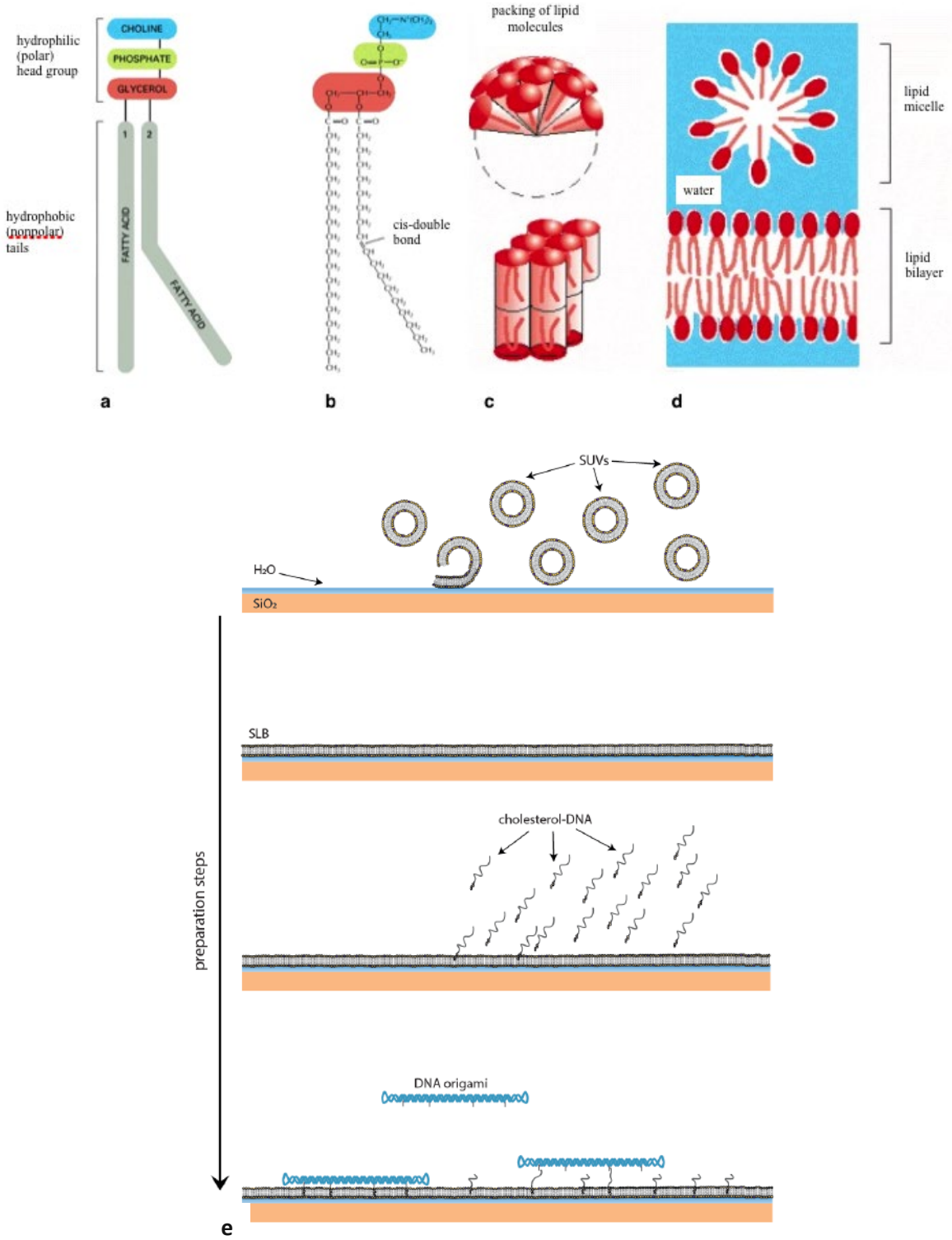


*Figure 6 Lipid Bilayer formation*

*The first two pictures are representations of the phospholipid phosphatidycholine a) schematically and b) by formula c) shows wedge-shaped and cylinder-shaped lipid molecules that form micelles and bilayers. In d) the cross section of a spontaneously formed micelle and bilayer in water is depicted. Images a-d adapted from [15]. e) shows the formation of a lipid bilayer on a hydrophilic surface [44].*



Die approbierte gedruckte Originalversion dieser Diplomarbeit ist an der TU Wien Bibliothek verfügbar
The approved original version of this thesis is available in print at TU Wien Bibliothek.
TU Bibliothek Your knowledge hub WIEN

For this work POPC, 1-palmitoyl-2-oleoyl-sn-glycero-3-phosphocholine, a phospholipid, was used for the creation of lipid bilayers. It contains an unsaturated fatty acid which reduces the melting temperature and leads to a liquid state at room temperature allowing for lateral diffusion of molecules or, in our case, DNA origami platforms anchored via cholesterol-modified oligonucleotides.

In order to bind the DNA origami to the lipid bilayer it is necessary to incubate cholesterol moieties. These moieties are elongated with the complementary DNA strand, Z, of the elongated strand Z' in the DNA origami platform *(Figure 6 (e))*.

## 1.2 Microscopy

Microscopy is one of the major tools when working in the fields of the life sciences. It enables the imaging of tiny object and areas of objects with a much higher resolution than the human eye is able to. Optical, electron and scanning-probe microscopy are the main three branches in the field. There are a lot of different techniques applicable in each of these branches. Depending on the size, the properties of the object and the aspects of it to be analyzed the appropriate technique has to be chosen. In this section I will describe the techniques used to image DNA origami.

### 1.2.1 Fluorescence Microscopy

One of many techniques in the field of optical microscopy is fluorescence microscopy. As this technique only, images fluorescent objects it is necessary to stain the DNA origami platforms with fluorophores. This has to be done with every object that is not auto fluorescent.

The fluorescent sample is up against a very dark background creating a high contrast enabling the imaging.

#### 1.2.1.1 Principles of fluorescence and microscopy setup

Fluorescence is the spontaneous emission of light by a substance after it has absorbed light. When light energy of a specific wavelength is absorbed by a fluorophore it gets excited. The absorbed light then gets reemitted at a longer wavelength therefore a lower energy.



Die approbierte gedruckte Originalversion dieser Diplomarbeit ist an der TU Wien Bibliothek verfügbar
The approved original version of this thesis is available in print at TU Wien Bibliothek.
TU Bibliothek Your knowledge hub WIEN

This energy loss can be shown by measuring the spectrum of excitation, which is similar to the absorption spectrum, and the spectrum of emission which is the fluorescent light emitted by the dye. A dye is characterized by its excitation maximum and by its emission maximum. The difference between these two maximum values is called Stokes shift. A useful way to describe this energy loss is by looking at a Jablonski diagram which demonstrates the orbitals which electrons can be in. When a dye absorbs light, an electron is brought into a higher orbital or energy state. Then through a process called internal conversion, the electron falls back to the lowest level of the excited state and then it will return its real ground state and emit a photon of a lower energy than the energy that was put in initially absorbed, which means that the emitted light is of a higher wavelength.

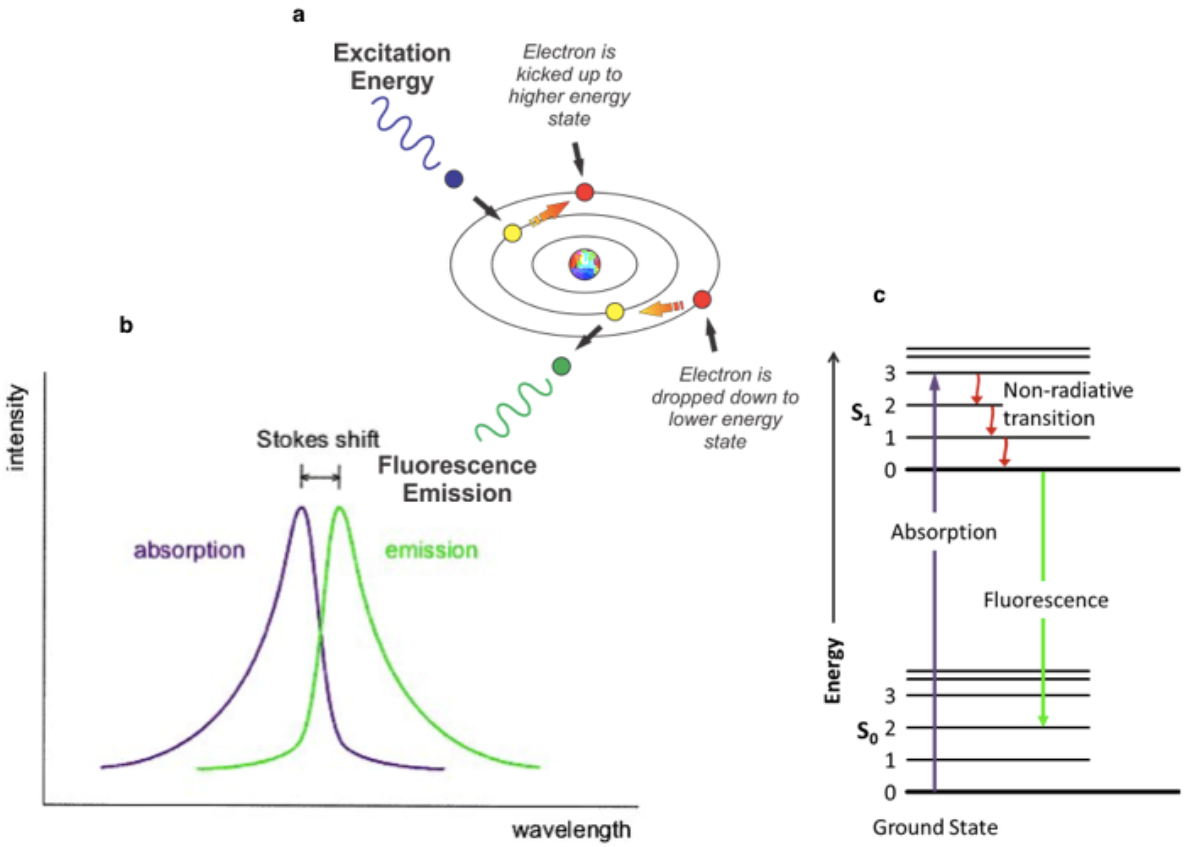


*Figure 7 Jablonski diagram and Stokes shift*

*a) An orbital electron is excited to a higher quantum state, when it relaxes back into its ground state a photon is emitted. [45] b) The Stokes shift describes the spectral shift between absorbed and emitted light [46] c) shows the Jablonski diagram with vibrational levels of fluorescence, non-radiative decay and absorbance [47]*

There are other possibilities that can occur as a result of this process than light emission, such as that the energy is transferred to other molecules or a non-radiative decay. The quantum



Die approbierte gedruckte Originalversion dieser Diplomarbeit ist an der TU Wien Bibliothek verfügbar
The approved original version of this thesis is available in print at TU Wien Bibliothek.
TU Bibliothek Your knowledge hub WIEN

efficiency describes the ratio between absorbed and emitted photons and as the Stokes shift its one of the main characteristics of fluorophores. The brightness of a dye is determined by how well it absorbs the excitation light (absorption coefficient) and what fraction of the excited state returns to the ground state under emission of fluorescence (quantum yield). Another important aspect is the lifetime of a fluorophore, which depends on the dye itself and on the environment. It is the time it takes to return to the ground state out of the excited state, which is usually in the order of nanoseconds. Fluorescent dyes only have a limited number of excitation/emission cycles they can go through, before the effect of photobleaching occurs. Photobleaching is the loss of fluorescence due to continuous light excitation over time. The size as well as the net charge of the fluorophore are further important parameters to be considered.

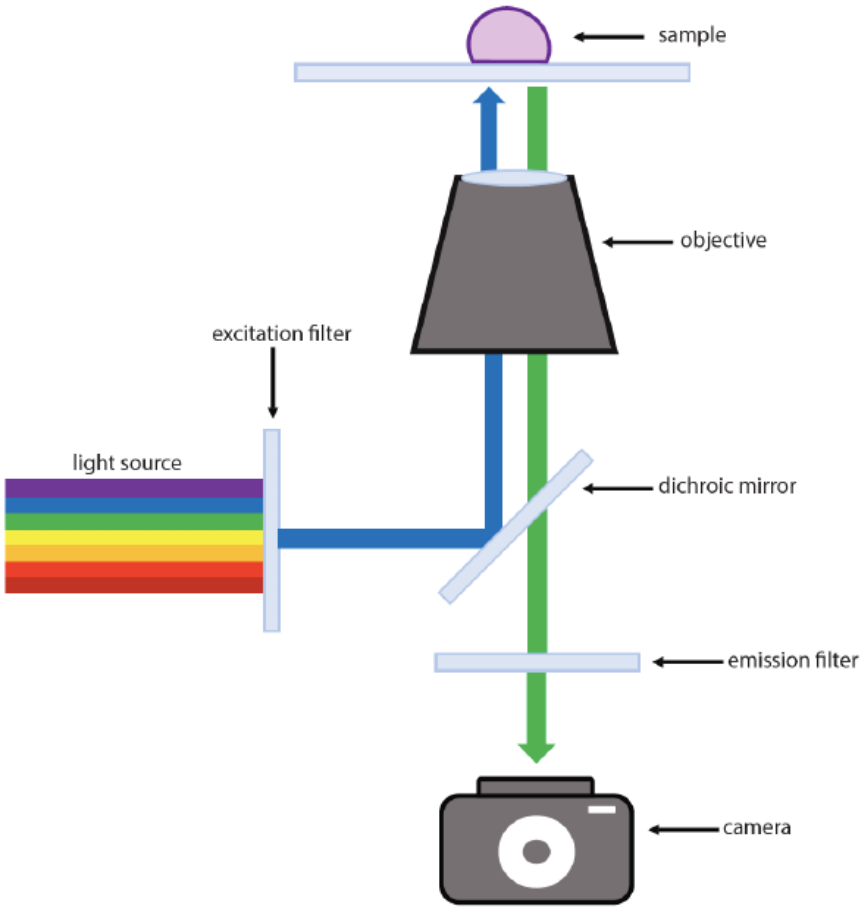


*Figure 8 Microscope scheme of components*

*The laser passes through an excitation filter, gets reflected by a dichroitic mirror and excites the fluorescence labeled sample which emits light that passes through the dichroitic mirror and through an emission filter. The emitted image then gets reflected towards a camera. [44]*

For the experiments an inverted fluorescence microscope was used. A laser with a wavelength close to the absorption maximum of the fluorophores was used to excite the sample (C). For



Die approbierte gedruckte Originalversion dieser Diplomarbeit ist an der TU Wien Bibliothek verfügbar
The approved original version of this thesis is available in print at TU Wien Bibliothek.
TU Bibliothek Your knowledge hub WIEN

this, the laser passes through an excitation filter (D) which only allows wavelengths to pass that are needed for emission. As a next step the filtered light gets reflected on a dichroic mirror (F), directing the laser beam towards the objective and the sample. The dichroic mirror only reflects a certain range of wavelengths and transmits other wavelengths. So, when the fluorophores get excited and emit light, it passes through the dichroic mirror and the emission filter (E), which blocks excitation light, towards the camera (A).

#### 1.2.1.2 Total internal reflection fluorescence (TIRF) microscopy

For the visualization of DNA origami bound to a lipid bilayer, total internal reflection fluorescence (TIRF) microscopy was used to avoid disturbing background signals and to only image a thin region at the bottom of the sample.

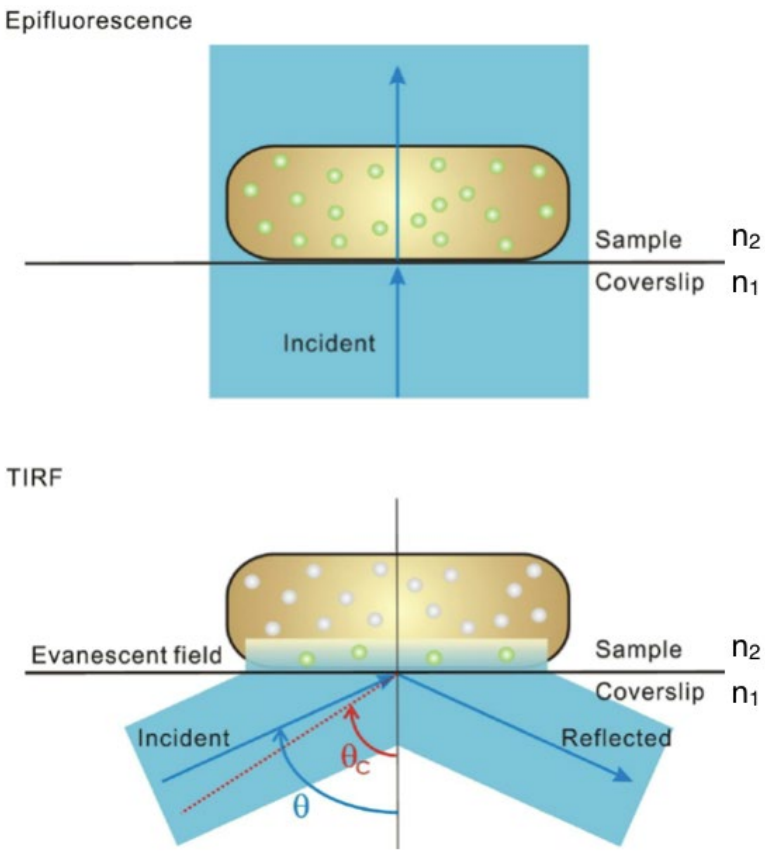


*Figure 9 Total internal reflective fluorescence microscopy*

*Depending on the angle (critical angle) in which the light enters the coverslip/sample interface, total reflection can occur. If that is the case, only fluorophores on the bottom of the sample get excited [48]*

Die approbierte gedruckte Originalversion dieser Diplomarbeit ist an der TU Wien Bibliothek verfügbar
The approved original version of this thesis is available in print at TU Wien Bibliothek.
TU Bibliothek Your knowledge hub WIEN

Total internal reflection occurs when light travels from an optically denser medium ($n_1$) such as glass to a less dense medium ($n_2$) such as an aqueous buffer solution if the incident angle is large enough. This effect can be described by considering Snell's law, representing the refraction of light at an interface:

$$n_1 \sin\theta_i = n_1 \sin\theta_t$$

$\theta_I$ describes the degree of incident and $\theta_t$ the angle of transmitted light. To calculate the critical angle $\theta_{critical}$ which denotes the smallest angle at which total internal reflection occurs $\theta_t$ is set to 90°C which means that the light beam does not enter the second material. The angle of incident or the critical angle can now be calculated:

$$\theta_i = \theta_{critical} = \sin^{-1}\left(\frac{n_1}{n_2}\right),\ n_1 > n_2$$

In order to be able to achieve the critical angle, an objective with a high numerical aperture has to be chosen.

#### 1.2.1.3 Single molecule fluorescence microscopy

Single molecule microscopy is a technique which enables the visualization of single fluorescently labeled molecules, locating their position with high accuracy and following their movements over time. The emission light from the fluorescent molecules is captured by an objective with a high numerical aperture, the measure of the photon collection capacity. The higher the numerical aperture the more emitted photons can be captured by the objective. This combined with a high amplification allows the visualization of individual molecules with a high resolution. Using the movies captured by the camera, it is possible to track individual particles and obtain information about the number and size of molecules, the diffusion coefficient and weather they are freely diffusing or confined within a certain area. The TIRF setup dramatically increases the signal to noise ratio. One can choose the desired frame size of the picture, the duration of the illumination as well as image acquisition and the time lag between subsequent images.

A point source such as a fluorophore emits spherical waves in concentric circles. The objective transfers the wave into plane waves which is intercepted by a tube lens and turns it back into a converging spherical wave.



Die approbierte gedruckte Originalversion dieser Diplomarbeit ist an der TU Wien Bibliothek verfügbar
The approved original version of this thesis is available in print at TU Wien Bibliothek.
TU Bibliothek Your knowledge hub WIEN

In order to understand many principles of microscopy it is necessary to understand the *Airy disc*. Resolution is the ability to distinguish objects that are separate from one another in reality in the sample as separate from one another in the image of the sample that is generated by the microscope. The resolution of an image is diffraction-limited.

When two light emitting fluorophores are too close to each other, a distance smaller than the minimal distance d, so that the resulting image does not show two clearly separated points, then the resolution is below the Rayleigh criterion. The minimal distance d between two light emitting points can be estimated by

$$d = 1.22 \cdot \frac{\lambda}{2n \cdot \sin\alpha}$$

where λ is the wavelength of the emitting light source, and $n \cdot \sin\alpha$ describes the numerical aperture.

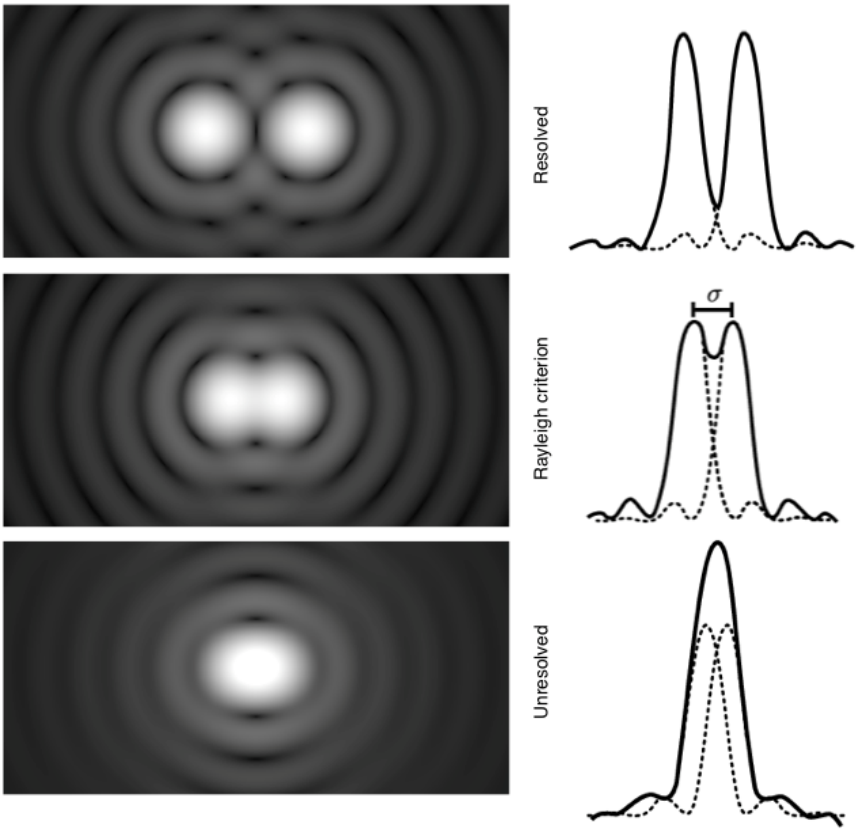


***Figure 10 Airy disc***

*The tree pictures on the left from top to bottom show two Airy discs at different distances to each other [49] in the image plane. The three pictures on the right show the corresponding intensity distribution. According to the Rayleigh Criterion two objects can just be resolved (top) if the diffraction maximum of one image coincides with the first minimum of another image. When two points are at a distance below the Rayleigh Criterion they cannot be resolved (bottom). Image adapted from [50]*



Die approbierte gedruckte Originalversion dieser Diplomarbeit ist an der TU Wien Bibliothek verfügbar
The approved original version of this thesis is available in print at TU Wien Bibliothek.
TU Bibliothek Your knowledge hub WIEN

The point spread function, the response of an imaging to a point source, can be approximated by a 2D Gaussian distribution. The precision for localization is given by

$$\Delta x = \frac{\sigma}{\sqrt{N}}$$

where Δx denotes the precision of the localization, σ the standard deviation from the PSF and N is the number of collected photons.

Further improvement of localization precision can be achieved by increasing the number of detected photons, a smaller pixel size than the standard deviation from the PSF, low surrounding background noise. The fluorophore densities should be low enough so that they can be distinguished individually.

The signal of a localized fluorophore can be fitted with a 2D Gaussian. By calculating the area under the curve, a brightness value for every fluorophore can be calculated as well.

#### 1.2.1.3.1 Single particle tracking

The spatiotemporal information gathered by the localization and tracking of single molecules is essential for mapping the diffusion behavior of molecules and small objects [51]. When the motion of particles is not affected in an active way by specific interactions and one can assume that the particles do not interact and only collide passively driven by thermal energy, the diffusion behavior of such particles can be described by Brownian motion. This was done by considering the mean squared displacement (MSD), which is a measure for the distance that a particle travels on average in a certain timespan. Random motions are not directionally oriented therefore the mean vectoral displacement around the starting point is zero, as the displacement in every direction has the same probability. However, most of the time experiments with single particle tracking do not show perfect Brownian motion but anomalous diffusion also called subdiffusion and superdiffuison. Subdiffusion describes the effect of slowed down long-range diffusion which can be the case for e.g. molecules diffusing on a cell membrane, whereas superdiffusion describes the effect of accelerated diffusion for example as a result of active transport processes in a cell.

The trajectories of single particles can be evaluated by localizing the single particles in each frame, assigning them coordinates and linking the frames by a nearest neighbor-algorithm. By using the calculated trajectories, the MSD is than used to determine the diffusion coefficient of the particle; further the type of diffusion can be inferred.



Die approbierte gedruckte Originalversion dieser Diplomarbeit ist an der TU Wien Bibliothek verfügbar
The approved original version of this thesis is available in print at TU Wien Bibliothek.
TU Bibliothek Your knowledge hub WIEN

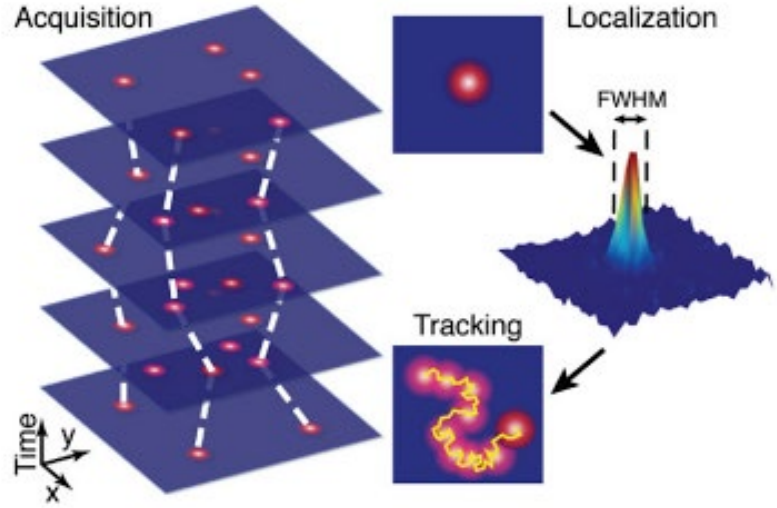


*Figure 11 Single Particle Tracking*

*In each individual acquired frame single particles (red points) are localized and at given timepoint their individual positions are determined in order to track single particles. [52]*

### 1.2.2 Atomic Force Microscopy

AFM is a technique in the field of scanning-probe microscopy. It has been developed in 1986 [53] and can be used for three major purposes: for measuring forces that occur between the probe and a sample, for imaging the topology of a surface and for manipulation of a sample. Since the resolution of an atomic force microscope is below 10 nm, I used AFM as topographic imaging tool in order to characterize the DNA origami platforms and analyze if they are folded in a correct manner.

#### 1.2.2.1 Fundamentals

A substantial part of the setup of an atomic force microscope is the cantilever. The forces acting between the sharp tip, also called probe, of a cantilever and a sample lead to bending and therefore deflections of the cantilever along the surface scanning process. These deflections are recorded by using the principle of light reflection. A laser is focused on the back of the cantilever, reflecting it towards a mirror which again reflects the laser beam towards two closely spaced photodiodes. Depending on the position where the reflected laser beam hits the diodes due to angular displacement of the cantilever one of the two diodes collects more light resulting in an output signal in relation to the cantilevers deflection. This is a highly sensitive method



Die approbierte gedruckte Originalversion dieser Diplomarbeit ist an der TU Wien Bibliothek verfügbar
The approved original version of this thesis is available in print at TU Wien Bibliothek.
TU Bibliothek Your knowledge hub WIEN

therefore it is necessary to avoid vibrations and noise while measuring, especially when the sample is of small magnitude.

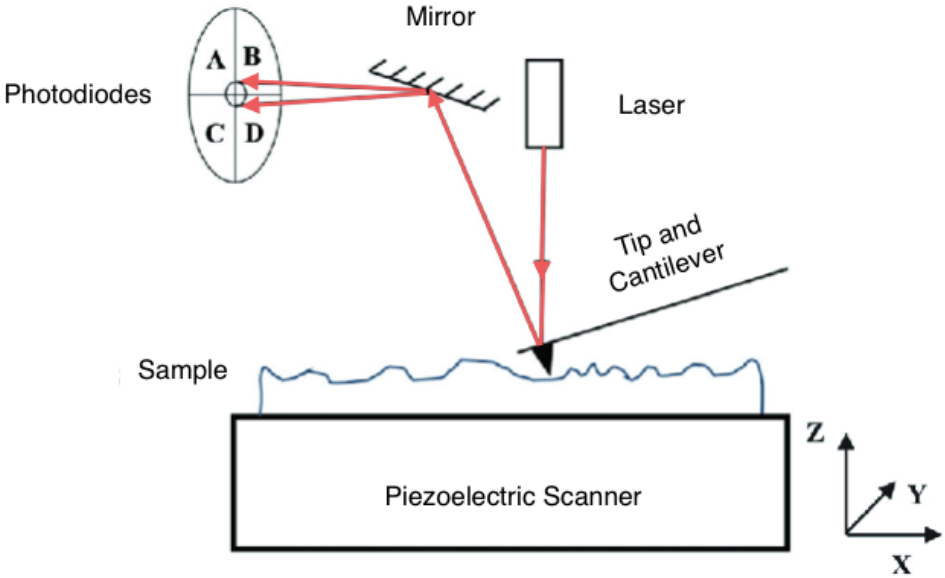


***Figure 12 Atomic Force Microscopy Setup***

*A schematic image of the principles of AFM. A laser is oriented towards the top of a cantilever which reflects the beam in relation to its movement towards a mirror which further reflects the laser beam towards light collecting photodiodes. The image was adapted form [54]*

The scanning process of the sample by the tip of a cantilever is driven by piezoelectric elements that move the probe relative to the sample. There are several imaging modes that can be used for measurement purposes depending on the properties of the sample to be analyzed. The three AFM modes of operation are: contact, non-contact and tapping mode. When using the contact ode, physical contact between the probe and the sample is achieved whereas when using the non-contact mode, the tip and the sample are at no point in direct contact. In non-contact mode resolution and scan speed are the lowest when compared to the two other modes, sample damage ca be avoided. For the work of this thesis he tapping mode was used. It allows for intermittent short contact between the probe and the sample. The scan speed and the resolution is highest at contact mode but damage of soft samples and image artefacts may occur.

Depending on the fragility of the sample as well as other factors one might be able to choose between different measurement environments such as vacuum, gas, air or liquid. For biological measurements it can be a huge advantage to measure in liquid as the sample is less prone to damage even when using contact mode. After fixating the DNA origami platforms on freshly cleaved mica the AFM measurements done as part of this thesis, have been carried out in liquid



Die approbierte gedruckte Originalversion dieser Diplomarbeit ist an der TU Wien Bibliothek verfügbar
The approved original version of this thesis is available in print at TU Wien Bibliothek.
TU Bibliothek WIEN Your knowledge hub

using an imaging buffer as well as in air. When measuring in liquid, one has to take under consideration that the laser beam travels through two mediums with different refractive indices, leading to a change of the angle of the laser beam. Therefore, the positions of the mirror and the photodiodes have to be changed accordingly.

After the imaging it is often necessary to process the images by subtracting the background or using filters to reduce noise and clarify the image resulting in a higher quality of analysis.

Die approbierte gedruckte Originalversion dieser Diplomarbeit ist an der TU Wien Bibliothek verfügbar
The approved original version of this thesis is available in print at TU Wien Bibliothek.
TU WIEN Bibliothek Your knowledge hub

# 2 Introduction

## 2.1 Project rationale

The work done for this thesis aims to contribute to a larger project by Emanuela Bianchi and Carina Karner (Institute of Theoretical Physics, TU Wien) called "Target delivery units from rectangular patchy particles". There, theoretical and numerical approaches are used to investigate the cumulative behavior of two-dimensional anisotropic patchy particles that have a fixed number of regions that attract each other but are overall repulsive [55]. By simulating self-assembly of asymmetric particles on surfaces they aim for the formation of loop-clusters with holes in the middle (open boxes) by assembling rectangular patchy building blocks before application as e.g. target delivery units. A simulation mimics the adsorption of two-dimensional platforms onto a substrate. By altering patch placements (Δ), number of components and energy level, combinations for achieving open box formation are examined. Therefore, a rectangle with the aspect ratio 2:1 was designed in six different ways to simulate four system classes. Patches are only placed on two sides of the rectangle either adjacent edges (adj) or in parallel (pl). There are four different types of patches (red (R), yellow (Y), blue (B) and green (G)) which attract (-ε) or repulse (+ε) each other according to the table in *Figure 9 b.)* resulting in four different classes: a one component (c) system with one type of patch (p) (1c1p), 2c2p, 2c3p and 3c3p.

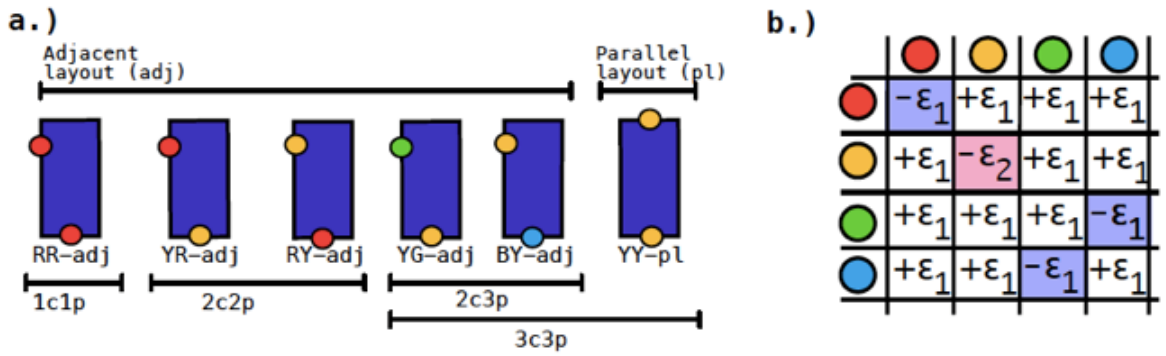


*Figure 13 Particle Types*

*In a.) the type of particles used for the simulation are depicted. Each particle has a different strategic patch placement for analysis of cluster formation. The table b.)shows the attraction/repulsion behavior between the patches. (Images courtesy of C. Karner)*

Die approbierte gedruckte Originalversion dieser Diplomarbeit ist an der TU Wien Bibliothek verfügbar
The approved original version of this thesis is available in print at TU Wien Bibliothek.
TU Bibliothek Your knowledge hub WIEN

While the assembly of a 1c1p system into an open box is a one step process the assembly of the other three systems is done in two steps, first one half and then the addition of the other half of the box. The two step processes are especially interesting because target delivery units can be filled into the partly formed boxes and then be closed.

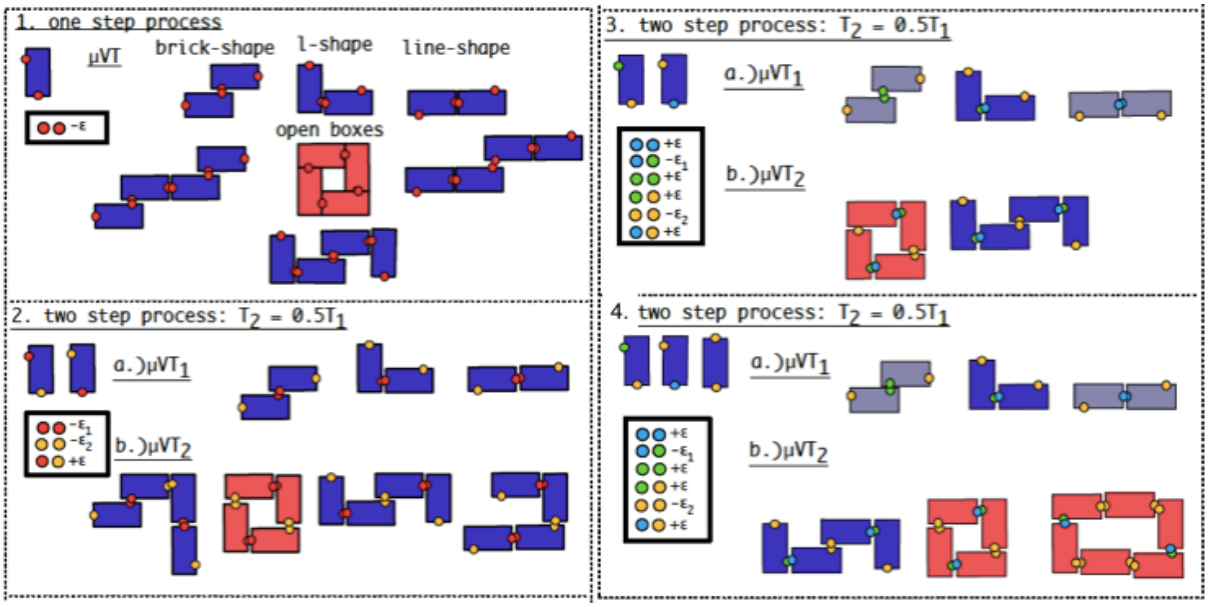


*Figure 14 Simulation Roadmap*

*Showing the effect of combinations of positive and negative interactions and different interaction strengths. (Images courtesy of C. Karner)*

In *Figure 10* the possibilities of different formations within the four systems are shown. In the first system many different formations of building blocks are possible. The 2c2p process allows for three different shapes after the first assembly step leading to four different building blocks in the second step. By refining system 2c2p and adding a different patch, the system 2c3p only allows for two different end products. And by extending the 3rd scenario with an additional component, three types of building blocks can be the result of a simulation, whereas two of them have the open box shape that the researches aim for. Altering the patch position on the long edges of the rectangles and the interaction strengths of the patches leads to very different results of the simulation. In the figure below one can see screenshot from a simulation run by working with the 1c1p system.

Die approbierte gedruckte Originalversion dieser Diplomarbeit ist an der TU Wien Bibliothek verfügbar
The approved original version of this thesis is available in print at TU Wien Bibliothek.

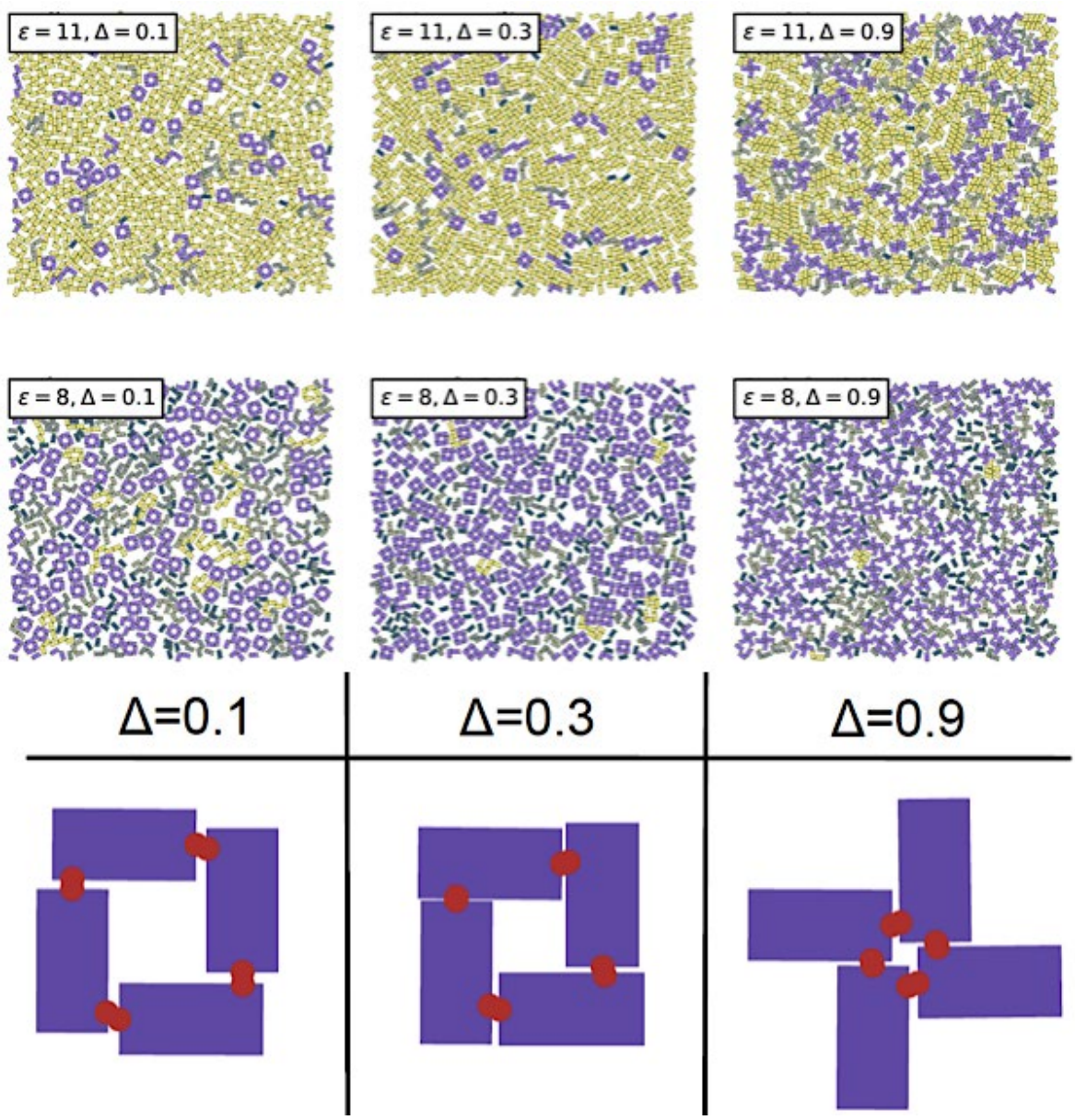


*Figure 15 Simulation Snapshots*

*Showing the effects of positioning of the interaction sites. (Images courtesy of C. Karner)*

## 2.2 Approach and Experimental Setup

The goal of this thesis was to make first attempts to reproduce the simulation in an analogue way. For this the following strategy was chosen: Rectangular patchy building blocks are designed by using DNA as a material and the method of DNA origami to form the DNA into a rectangle with the aspect ratio 2:1. For interaction between two platforms, short DNA strands were designed that bind to specific unpaired bases in the DNA origami structure on one end



Die approbierte gedruckte Originalversion dieser Diplomarbeit ist an der TU Wien Bibliothek verfügbar
The approved original version of this thesis is available in print at TU Wien Bibliothek.
TU Bibliothek Your knowledge hub WIEN

and hang loose on the other end (interaction strands). To achieve this on the short edges, specific bases on the scaffold strand were left unpaired by staple strands for further binding with the interaction strands. On the long edges, the scaffold strand forms hairpins leaving bases for the binding with interaction strands. Interaction between individual DNA origami platforms is the initiated by addition of binding strands, complementary singe strands, designed in a way to connect two DNA origami platforms at those lose hanging ends of the DNA strands attached to the edges of the scaffold strand. This strategy has the main advantage that it allows to i) initiate platform assembly at will by addition of connector strands and ii) control the interaction strength via the number of paired bases that connect two platforms.

As substrate used for the platforms to adsorb onto, a supported lipid bilayer on a glass coverslip was chosen.

In the computational design process a rectangle with the aspect ratio 2:1 was created. By applying some basic rules described in the introduction, one can ensure that the design correctly folds when preparing it in the laboratory. The chosen platforms size was 50 x 100 nm and it was 2 nm high, the width of a DNA double helix.

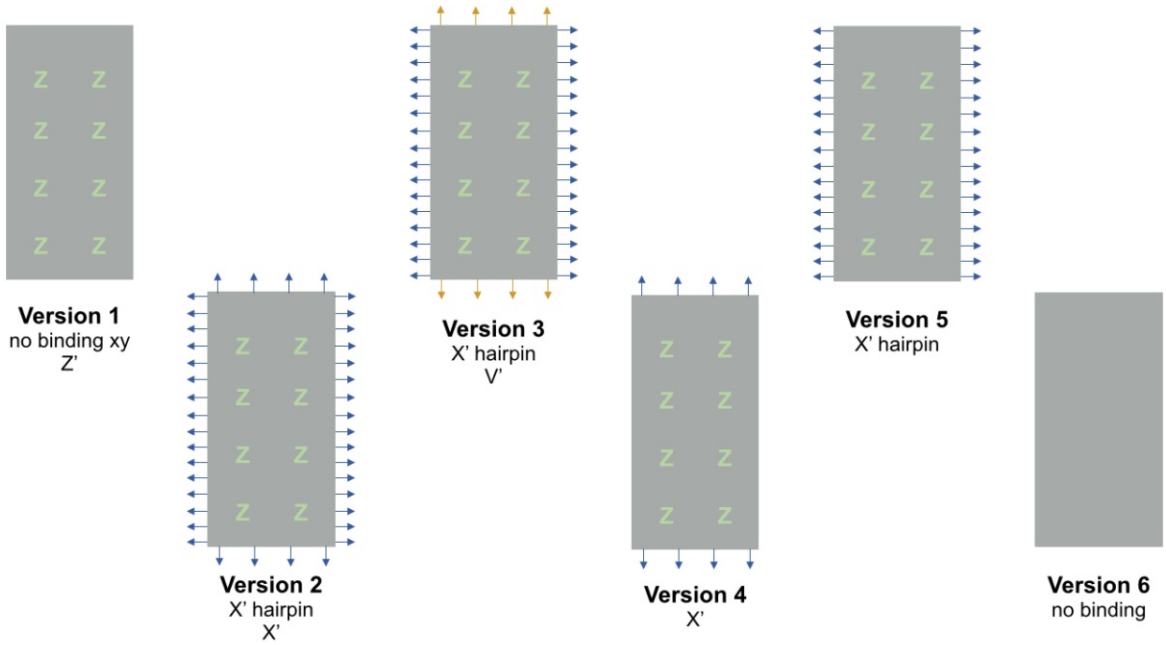


*Figure 16 Six Versions of DNA origami structures with different placements of strands for interaction*

*Version 1: only binding to lipid bilayer possible, Version 2: binding with lipid bilayer and between X' hairpin strand on the long edges and between X' strands on the short edges possible, Version 3: binding with lipid bilayer and binding between X' hairpin strand on the long and V' strand on the short edges possible, Version 4: binding with lipid bilayer and binding between X' strands on the short edges, Version 5: binding with the lipid bilayer and between X' hairpin strands on the long edges possible,, Version 6: no possible binding*



Die approbierte gedruckte Originalversion dieser Diplomarbeit ist an der TU Wien Bibliothek verfügbar
The approved original version of this thesis is available in print at TU Wien Bibliothek.
TU Bibliothek Your knowledge hub WIEN

In order to recreate the simulations described in the previous section *Project rationale* only two to three hybridization strands would have been necessary to recreate one patch, but to allow flexible placement of interaction sites the 6 different versions depicted in *Figure 16* were designed. Version 1 and 6 serve as reference, version 2 and 3 allow for binding on every edge of the platforms and version 4 and 5 were designed to facilitate the visualization via fluorescence microscopy due to the building of linear aggregates.

The design includes eight staple strands, that can be elongated for attachment of cholesterol-modified strands to bind the DNA origami platform to a planar supported lipid bilayer (SLB). Further four staple strands on each short side and 16 staple strands on each long side of the rectangle can be elongated for binding between platforms. Due to the variability of the elongations, six different versions of such DNA origami rectangles were created for the analysis of their oligomerization behavior.

Elongated strands towards the yz-plane, are further called Z'-strands, elongated strands on the long edges of the platform pointing outwards in the xy-plane are always called X' strands and depending on the version discussed, the elongated strands on the short edges of the platform are either described by X' (blue) as well or by V' (yellow).

Die approbierte gedruckte Originalversion dieser Diplomarbeit ist an der TU Wien Bibliothek verfügbar
The approved original version of this thesis is available in print at TU Wien Bibliothek.
TU Bibliothek Your knowledge hub WIEN

# 3 Material and Methods

## 3.1 Computational design of the DNA Origami

Before actually preparing the DNA origami platforms in the laboratory, the rectangular DNA origami was designed. This was realized by using the following open source tools:

- caDNAno used for the design of the platform,
- CanDo used to analyze the design,
- Maya: vHelix used for the visualization of strands to be elongated,
- NUPACK used for the analysis of strand behavior.

The open source software caDNAno [36] was used to design a rectangle with an aspect ratio 2:1. After identifying the number of helices and bases needed for the rectangular shape the scaffold strand was placed accordingly. For the addition of the staple strands the rules described in the introduction were applied. In order to reduce stress and strain within the platform, bases were skipped in a symmetrical manner.
For the visualization of the sites chosen to be elongated for binding either to the lipid bilayer or to other DNA origami platforms the Maya vHelix plugin [56] was used, making sure that the elongations point towards the wanted directions.
For computational analysis of the mechanical properties and the incorporation efficiency, the free online resource CanDo [37], [38] was used.
The NUPACK website [57] was used to design the binding strands enabling the interaction between different platforms and a platform and the lipid bilayer.

## 3.2 Preparation of DNA Origami

In this part of the thesis I will describe how to get from over 100 single DNA-strands to a folded rectangular DNA origami platform by exploiting the physical, chemical, thermodynamic and



Die approbierte gedruckte Originalversion dieser Diplomarbeit ist an der TU Wien Bibliothek verfügbar
The approved original version of this thesis is available in print at TU Wien Bibliothek.
TU Bibliothek Your knowledge hub WIEN

mechanical properties of DNA and standard laboratory equipment. I will further present two methods to analyze the quality of the folded platforms.

### 3.2.1 DNA origami folding buffer conditions

For the folding process of DNA origami, a folding buffer was needed to support efficient structure formation. In this work a folding buffer composed of:

- tris(hydroxymethyl)aminomethane Tris 50mM
- natrium chloride NaCl 500mM
- ethylenediaminetetraacetic acid EDTA 10mM
- magnesiumchloride $MgCl_2$ 100mM

As $MgCl_2$ forms a chelate with EDTA it was stored separately.
For the production of the *Mastermix* needed for the folding process the DNA-strands were available at concentrations of 50µM and dissolved in TE buffer, to stabilize the DNA and protect it from degradation.

### 3.2.2 Folding of DNA origami and addition of interaction strands

In this case, a Polymerase Chain Reaction (PCR) machine was used as a thermal cycler to facilitate the thermal annealing process of the DNA. Before the PCR, a *Mastermix,* of the DNA staple strands for each of the 6 versions of the DNA origami platforms, was created. In the case of this work, *Mastermix 1(see appendix)* and *Mastermix 2 (se appendix)* consisted of 52 different staple strands each. Depending on the platform to be folded, the needed supplementary staple strands and elongated strands were added in a next step.
Before folding the DNA origami, the right concentration of staple strands, scaffold strands, folding buffer, modified staple strands, $MgCl_2$ and water was calculated depending on their concentrations. Whereas the final concentration of each DNA strand of unmodified staple strands should be tenfold [58] of the scaffold strand, the final concentration of each modified DNA strand should be 50 times higher.



Die approbierte gedruckte Originalversion dieser Diplomarbeit ist an der TU Wien Bibliothek verfügbar
The approved original version of this thesis is available in print at TU Wien Bibliothek.
TU Bibliothek Your knowledge hub WIEN

| Components | Concentration | # Strands | Concentration per DNA-Strand | Amount (µl) | Final Concentration |
|---|---|---|---|---|---|
| Version 1: no binding xy, Z' | | | | | |
| *Scaffold Strand* | 100 nM | | | 10 | 10nM |
| *Folding Buffer* | 10x | | | 10 | 1x |
| *MgCl_2* | 100 mM | | | 12.5 | 12.5mM |
| *Mastrermix 1* | 50,000 nM | 52 | 962 nM | 10.4 | 100 nM per Strand |
| *Mastrermix 2* | 50,000 nM | 52 | 962 nM | 10.4 | 100 nM per Strand |
| *Z' Mix* | 100,000 nM | 8 | 12,500 nM | 0.8 | 100 nM per Strand |
| *No binding xy* | 50,000 nM | 8 | 6,250 nM | 1.6 | 100 nM per Strand |
| *UP H2O* | | | | 44.3 | |
| **Total** | | | | **100** | |
| Version Mix 3: X' hairpin, V' | | | | | |
| *Scaffold Strand* | 100 nM | | | 10 | 10nM |
| *Folding Buffer* | 10x | | | 10 | 1x |
| *MgCl_2* | 100 mM | | | 12.5 | 12.5mM |
| *Mastrermix 1* | 50,000 nM | 52 | 962 nM | 10.4 | 100 nM per Strand |
| *Mastrermix 2* | 50,000 nM | 52 | 962 nM | 10.4 | 100 nM per Strand |
| *Z' Mix* | 100,000 nM | 8 | 12,500 nM | 0.8 | 100 nM per Strand |
| *X' Mix* | 100,000 nM | 8 | 12,500 nM | 0.8 | 100 nM per Strand |
| *UP H2O* | | | | 45.1 | |
| **Total** | | | | **100** | |

***Table 1 DNA Origami Version 1 and Version 3***

*This table shows the components and their quantities mixed together in order to get 100µl of DNA origami folding mix for each version (version 1 and version 3).*

For the folding process 10 µl of the 100 µl DNA origami mix were filled into ten small premium PCR tubes and then put in the PCR machine. By heating up the sample from room temperature to 90°C at 10°C per minute and 15 minutes of incubation, secondary structures of the scaffold strand opened up making it free for staple strands to attach. For this, the sample was cooled down 1°C per minute down to 4°C.



Die approbierte gedruckte Originalversion dieser Diplomarbeit ist an der TU Wien Bibliothek verfügbar
The approved original version of this thesis is available in print at TU Wien Bibliothek.
TU Bibliothek Your knowledge hub WIEN

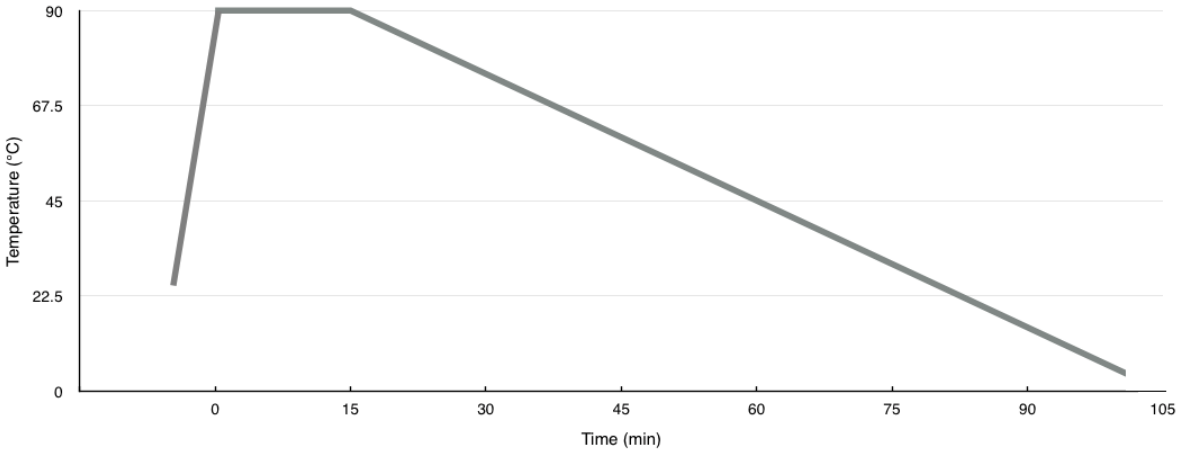


*Figure 17 PCR temperature profile*

*A graph of the temperature profile of the folding process. The DNA origami mix is heated up to 90°C to be cooled down slowly to 4°C.*

As an excess of staple strands has been added in the beginning of the process and it can be assumed that the DNA origami folded correctly, the sample still contained a surplus of staple strands. These short strands were to be filtered by using spin column purification.

In cases where 3.2 µl of 100 mM interaction strands were added to the DNA origami platforms after purification the samples were incubated for 60 minutes at 37°C and 300 rpm and cooled down 1°C per minute to 10°C before being purified.

### 3.2.3 Spin Column Purification

For filtering out excessive DNA strands Amicon Ultra – 0.5 with a 100K membrane filters were put into an Eppendorf tube. First 500µl of folding buffer containing 5mM of $MgCl_2$ were evenly distributed onto the filter and put into the centrifuge to spin for 5 minutes at 5.000G.
When done, the filtered liquid was removed from the tube and the filter reinserted. Then, as a second step, 100µl of the DNA origami was mixed with 400µl of the FoB- $MgCl_2$ solution and evenly distributed on the filter. The tubes were again put into the centrifuge for 5 minutes at 7,000G.
The third step was repeated by removing the liquid in the bottom of the tube, adding 500µl of the FoB- $MgCl_2$ mix and spin the sample at 7,000G for 5 minutes.



Die approbierte gedruckte Originalversion dieser Diplomarbeit ist an der TU Wien Bibliothek verfügbar
The approved original version of this thesis is available in print at TU Wien Bibliothek.
TU Bibliothek Your knowledge hub WIEN

Then the filter was flipped over and put in a new Eppendorf tube containing 81µl of the FoB-$MgCl_2$ solution to end up with a final volume of 100 µl. The open Eppendorf tube with the flipped filter was then centrifuged again for 4 minutes at 5.000G.
The remining 100 µl mixture contained the filtered DNA origami structures and could either be stored in a freezer at -20°C or immediately used.

## 3.3 Quality control and characterization of DNA Origami

### 3.3.1 Gel Electrophoresis

In order to separate DNA fragments according to their size and therefore characterize the DNA origami platforms, the method of gel electrophoresis was used.
For the gel production, 0.5 g of Agarose was mixed with 50 ml of TAE-buffer, a solution containing EDTA, tris base and acetic acid. After gently shaking the flask the mixture was put into the microwave at 800W and heated up until the liquid starts to bubble. This process was repeated until the liquid gets clear. Then the solution was cooled down to ~45°C by turning the flask under running water. After adding 5 µl of Sybr-Gold DNA gel-stain the liquid gel was put into the plastic pan, in which the electrophoresis took place, and the plastic comb, for insertion of the sample, was put into the pan. After 20 to 30 minutes the gel got solid, had a milky surface color and was ready for the loading of the samples into the wells created by the comb.

For the preparation of the samples to be put into the wells in the gel created by the plastic comb, DNA origami were mixed with TE buffer solution and a loading dye (purple 6x no SDS (sodium dodecyl sulfate). The same was done with the scaffold strand for comparison and additionally two different DNA Ladders, FastRuler Middle Range DNA Ladder and GeneRuler 1kB DNA Ladder, mixed with TE buffer for measurement purpose. In the following table the exact amounts of compounds for the mixes can be found.

Die approbierte gedruckte Originalversion dieser Diplomarbeit ist an der TU Wien Bibliothek verfügbar
The approved original version of this thesis is available in print at TU Wien Bibliothek.
TU Bibliothek Your knowledge hub WIEN

| | | TE Buffer | Purple 6x no SDS |
|---|---|---|---|
| **DNA origami version** | 3µl | 21µl | 4µl |
| **Scaffold Strand** | 0.3µl | 23.7µl | 4µl |
| **FastRuler Middle Range DNA Ladder** | 5µl | 20µl | |
| **GeneRuler 1 kB DNA Ladder** | 0.7µl | 22.5µl | |
| **TriTrac** | 1µl | | |

*Table 2 Loading samples for the Gel Electrophoresis*

*This table indicates the components and amounts used to fill a gel electrophoresis pocket with a volume up to 25µl.*

The gel electrophoresis was run for 90 min at 70V and the DNA fragments moved through the gel with a speed according to their size, smaller fragments faster than larger fragments, leading to a clear separation. The DNA fragments could then be observed as bands, representing groups of same sized fragments.

### 3.3.2 Concentration measurement

Thermo Scientific Varoskan (ThermoFisher) is a microvolume spectrometer and fluorometer for DNA, RNA and protein quantitation. After cleaning the µDrop plate (ThermoFischer) the concentration of the double stranded DNA in the sample was determined by pipetting 2µl of the buffer and the sample on the designated black spots on the Synergy H1 microplate and inserting it into the microplate reader. The application GEN5 2.03 was used to start the analyzing process. Therefore, one had to choose the desired molecule to be determined, in this case double stranded DNA (dsDNA), and mark the individual spots where the samples and the buffer were placed. The buffer concentration was subtracted from the density value of the investigated samples resulting in the concentration value of the double stranded DNA in the sample. The measured values are then exported into an Excel file.

### 3.3.3 Atomic Force Microscopy

#### 3.3.3.1 Sample preparation

For the preparation of the sample used for the atomic force microscopy a piece of mica was punched out, cleaved and glued onto a cover slip by using Norland Optical Adhesive 68 glue



Die approbierte gedruckte Originalversion dieser Diplomarbeit ist an der TU Wien Bibliothek verfügbar
The approved original version of this thesis is available in print at TU Wien Bibliothek.
TU Bibliothek Your knowledge hub WIEN

and exposing it to UV light for curing. Then the mica was cleaved using adhesive tape and the process was repeated until the surface of the mica is even.

Then the AFM imaging buffer consisting of 40mM Tris, 2mM EDTA and 12.5mM $MgCl_2$ was incubated on the flat mica surface for 5 minutes. Then 3µl of purified 4.5 nM DNA origami solution was added and incubated for 30 minutes. As a last step more AFM imaging buffer was added to the sample enclosed by a chamber formed out of two-component dental glue.

#### 3.3.3.2 Instrument and settings

A NanoWizard 3 from JPK instruments was used in tapping mode for imaging. MSNL 10 E cantilevers (Bunker) were used having a resonance frequency of 26 – 50kHz and a spring constant of 0.1N/m. After calibration in water, the spring constant was measured to be 0.072N/m and the resonance frequency was 7.7kHz. The relative setpoint was set to be as high as possible which was at 72%. This was also achieved by augmenting the drive amplitude to 0.4V. Depending on the scanning region the scanning speed was adapted. For smaller regions the line rate was increased. As postprocessing steps a polynomial surface is subtracted and the height profile range of interest was accentuated.

## 3.4 Supported Lipid Bilayer Production

### 3.4.1 Production of lipid vesicles

For the production of POPC vesicles Schott Fiolax vials were used. The five-fold of vesicle concentration was produced by using 50µl of POPC (10mg/ml) therefore 0,5mg of lipids dissolved in chloroform. For the evaporation of the chloroform a constant low nitrogen stream was held on the solution for about 15 minutes. 1 ml of Phosphate Buffered Saline (PBS) 10x was added to the dried solution, the vial was sealed with parafilm and then vortexed until the solution gets unclear. The sealed vial was then put into the sonication bath to allow unilamellar vesicles to form. One had to ensure that once the vial is in the rippling bath that the liquid in the tube is mixed for 10 to 20 minutes due to sonication waves. After this process the solution could be stored in the fridge at 4°C for 3-5 days.



Die approbierte gedruckte Originalversion dieser Diplomarbeit ist an der TU Wien Bibliothek verfügbar
The approved original version of this thesis is available in print at TU Wien Bibliothek.
TU Bibliothek Your knowledge hub WIEN

### 3.4.2 Production of supported lipid bilayer

For SBL production the lipid vesicle solution solution was diluted 1:5 with PBS 10x. For the preparation of SBL a Labtek chamber had to be prepared. Therefore, the Labtek chamber was cleaned with ethanol and a two-component dental glue was used to glue freshly plasma cleaned glass cover slips onto the chamber.

As soon as the glue solidified, 150µl of the POPC vesicle solution were added into each well of the Labtek chamber and incubated for 10-15 minutes for bilayer formation. The excess of vesicles was gently washed out with 15ml 1x PBS. At least 200µl 1x PBS was kept in each well for imaging.

### 3.4.3 Addition of DNA-cholesterol anchors

The Z-cholesterol strands were mixed with 1x PBS. 0,25µl of 50mM Cholesterol and 19,75µl of 1x PBS were added to each well of the Labtek chamber and incubated for 1 hour followed by a washing step of each well with 5ml PBS.

### 3.4.4 Labeling and addition DNA origami

For labeling DNA origami 1mM YOYO-1™ (YOYO) was used. First YOYO was diluted with TE buffer (10 mM Tris, 1mM EDTA) in the ratio 1:1000 to concentration of 1 µM. Then 80µl of this mix and 80µl of the 4.5 nM DNA origami were mixed together, spun down and put in the Thermomixer for 45 minutes at 24°C and 3000 rounds per minute. After this process the DNA origami-YOYO mix was purified by using the spin column purification method described in the subsection 2.2.3. 17µl of 1.625 nM DNA origami solution was added to a well of the Labtek chamber containing a lipid bilayer and DNA-cholesterol strands. The sample could either be stored immediately or stored in the fridge for 24h at 4°C.

Die approbierte gedruckte Originalversion dieser Diplomarbeit ist an der TU Wien Bibliothek verfügbar
The approved original version of this thesis is available in print at TU Wien Bibliothek.
TU Bibliothek WIEN Your knowledge hub

## 3.5 Total Internal Reflection Fluorescence Microscopy

For the experiments TIRF microscopy was performed on a system built based on a Zeiss Axiovert 200 microscope. The microscope was equipped with a Zeiss 100x, NA = 1.46 Plan-Apochromat objective. A motorized table shifted the mirror so that the excitation beam was parallel to the optical axis in order to achieve TIR illumination. Three laser lines were overlaid and their intensity and timing modulated.

A dichroic mirror (Semrock) separated the emission and excitation spectra. By using and Optosplit 2 image splitter (Oxford Instruments) containing a further dichroic mirror (Semrock) and an emission filter per color channel (Chroma), the signals emitted were split into two color channels and imaged on a CCD camera (iXon ultra 897, Andor).

### 3.5.1 Diffusion Coefficient

A MATLAB algorithm (S. Wieser, M. Moertelmaier, E. Fuertbauer, H. Stockinger, G. J. Schütz, (Un)confined diffusion of CD59 in the plasma membrane determined by high-resolution single molecule microscopy. Biophys. J. 92, 3719–3728 (2007))[44] was for the mobility analysis of DNA origami. At different locations on the supported lipid bilayer 100 images sequences were recorded at a time lag of 15ms and an illumination time of 5 ms. In order to determinate the diffusion coefficient (D), the function $MSD = 4Dt+4\sigma_{xy}$ was fitted. Therefore, the mean-square displacements (MSDs) were averaged over the trajectories. $\sigma_{xy}$ is the localization precision. The first and the second data point of the MSD plot were used to determine the diffusion coefficients.

### 3.5.2 Oligomerization

After adding 5µl of the corresponding binding strands (50 mM) into the wells of the Labtek chambers containing DNA origami on lipid bilayers and incubating the sample for 30 minutes at 37°C oligomers started to form. The yield of formed oligomers as well as their size were evaluated using TIRF microscopy.



Die approbierte gedruckte Originalversion dieser Diplomarbeit ist an der TU Wien Bibliothek verfügbar
The approved original version of this thesis is available in print at TU Wien Bibliothek.
TU Bibliothek Your knowledge hub WIEN

# 4 Results and Discussion

## 4.1 Computational design of DNA origami rectangles

For the design of DNA origami rectangles with an aspect ratio 2:1 the state-of-the-art open source software caDNAno[36] was used. Three versions have been finalized having the sizes of 100*50nm, 50*100nm and 30*60nm. For the design of the layout of the scaffold strand the procedure was the same for all three versions: calculate the number of helices needed to achieve the wanted width of the rectangle and calculate the bases needed in a row to achieve the wanted length of the rectangle. As the number of helices $h$ can only be an integer number, the wanted width has to be approximated. One helix has a diameter of 2 nm and between the helices there is a gap of 1nm [3]. Therefore, the number of helices $h$ for a wanted width $w$ can be approximated as follows:

$$h * 2 + (h - 1) \approx w.$$

As in the caDNAno template 16 base pairs represent 1.5 helical turns and 3 turns are 10.8nm long [3] the approximate number of base pairs $bp$ corresponding to the wanted length $l$ can be calculated by

$$l/10.8nm * 32bp = bp.$$

Then as a next step the long single scaffold strand was folded by placing $h$ strands along the y-direction of the wanted shape and connecting them to each other so that together they form one long scaffold strand. This is only possible at specific sites where the tangent of the DNA twist points towards the strand to be connected which is possible every odd number of half turns. As the design process of DNA origami is facilitated when designed in a symmetrical manner, the seam was placed to be in the middle of my design. The third step, the design of the staple strands, is rendered by the software. As with DNA in general, it is important to consider the directionality of the scaffold and the staple strands. Now that the staple strands are placed by the software, they have to be adapted. For example, the rule for the length of such staple strands is that they should be longer than 16 bases to ensure stability of duplex formation but no longer than 50 bases because of the higher cost and increased duration of incorporation [3]. Further it



Die approbierte gedruckte Originalversion dieser Diplomarbeit ist an der TU Wien Bibliothek verfügbar
The approved original version of this thesis is available in print at TU Wien Bibliothek.
TU Bibliothek Your knowledge hub WIEN

is recommended to avoid staple strands at the edges of the design as this may lead to large-scale aggregation [3]. Another rule to follow is that the breaking points of staples should be further than four bases away for crossovers and that a staple strand should at least cover eight bases in one row before crossing over to another row [3][36]. By crossing over to a next row, the staple strand changes direction. For the purpose of reducing stress and inducing flexibility it is possible to intentionally skip bases and leave them unpaired [59].

Die approbierte gedruckte Originalversion dieser Diplomarbeit ist an der TU Wien Bibliothek verfügbar
The approved original version of this thesis is available in print at TU Wien Bibliothek.
TU WIEN Bibliothek Your knowledge hub

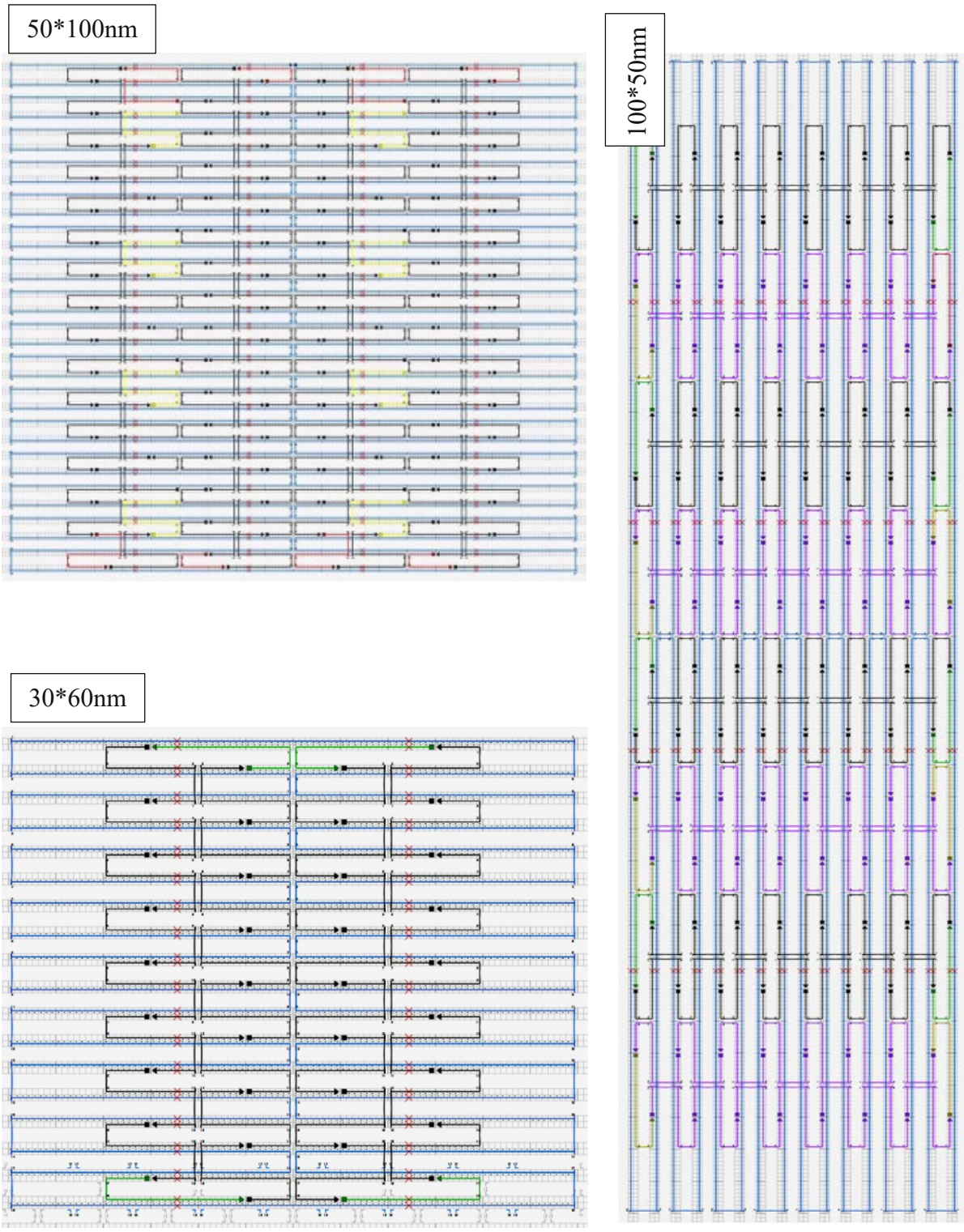


*Figure 18 Finished caDNAno Designs*

*Three different examples of platforms designed with the caDNAno software: 50x100, 100x50 and 30x60 nm. 50x100nm: the yellow staple strands indicate binding sites towards the z-direction for attachment to a lipid bilayer and the red staple strands on the short edges represent binding sites towards the xy-plane for interaction between platforms. The red crosses indicate skipping of bases to reduce the stress acting on the platform. In every row 16 bases next to the long edges were left unpaired resulting in hairpin-like structures. These will further be used to attach interaction strands. 30*60 and 100*50 nm: the colors of the staple strands were chosen randomly.*



Die approbierte gedruckte Originalversion dieser Diplomarbeit ist an der TU Wien Bibliothek verfügbar
The approved original version of this thesis is available in print at TU Wien Bibliothek.
TU Bibliothek Your knowledge hub WIEN

After editing the staple strands, interaction strands to be elongated were placed and their 3' ends were positioned to be pointing outwards towards the wanted directions. Therefore, the strands that are supposed to interact with a lipid bilayer, 8 strands when working the 100*50nm and 50*100nm layout and 6 when using the 30*60nm layout, were positioned to point in axial and strands that will interact with other platforms point at lateral position of the platform. The Maya v-helix plugin was used for the visualization of the directed interaction strands.

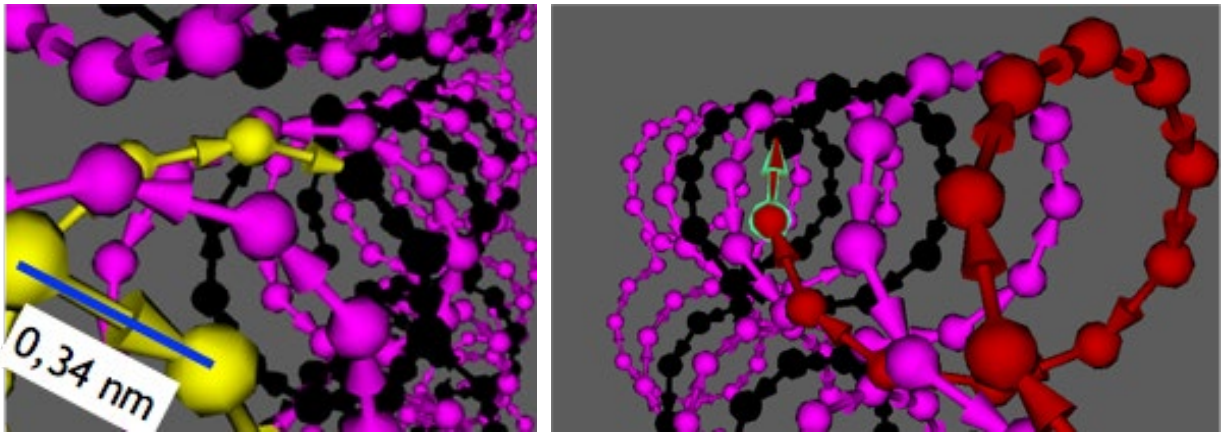


***Figure 19 vHelix visualization***

*The two pictures show parts of a simulated folded DNA origami platform. The scaffold strand is represented in pink, the staple strand to be elongated for interaction between platforms is indicated in red, a staple strand to be elongated for binding to a lipid bilayer is depicted in yellow and other staple strands in black. Most important, the directionality of each strand is indicated.*

CanDo [37], [38] was used for model prediction. Using a finite-element-based modeling approach, CanDo performs 3D model prediction using the design files from caDNAno [36]. As an output the values for the minimum root mean square fluctuation (RMSF), 95% RMSF and maximum RMSF as well as heatmaps form several perspectives are provided. Whereas blue describes a low and red a high relative flexibility. The RMSF was used as indicator [60] for the incorporation efficiency which strongly varies between the different positions on a DNA origami platform. The lower the RMSF the better the strand incorporation efficiency of the DNA origami platform. The bluest color in the plot represents the 0 % RMSF and the reddest stands for higher than 95 % RMSF.

Die approbierte gedruckte Originalversion dieser Diplomarbeit ist an der TU Wien Bibliothek verfügbar
The approved original version of this thesis is available in print at TU Wien Bibliothek.
TU Bibliothek Your knowledge hub WIEN

| | Minimum RMSF | 95% RMSF | Maximum RMSF |
|---|---|---|---|
| 50*100nm | 0.439nm | 1.820nm | 3.233nm |
| 100*50nm | 1.084nm | 3.467nm | 4.983nm |
| 60*30nm | 1.073nm | 3.237nm | 4.333nm |

***Table 3 RMSF for different DNA origami platforms***

*This table shows the minimum RMSF, the 95% RMSF and the maximum RMSF of each of the computationally designed platforms: 50x100nm, 100x50nm and 60x30nm. The value is to be seen in relation to the size. The lower the RMSF the higher the probability of correct strand incorporation.*

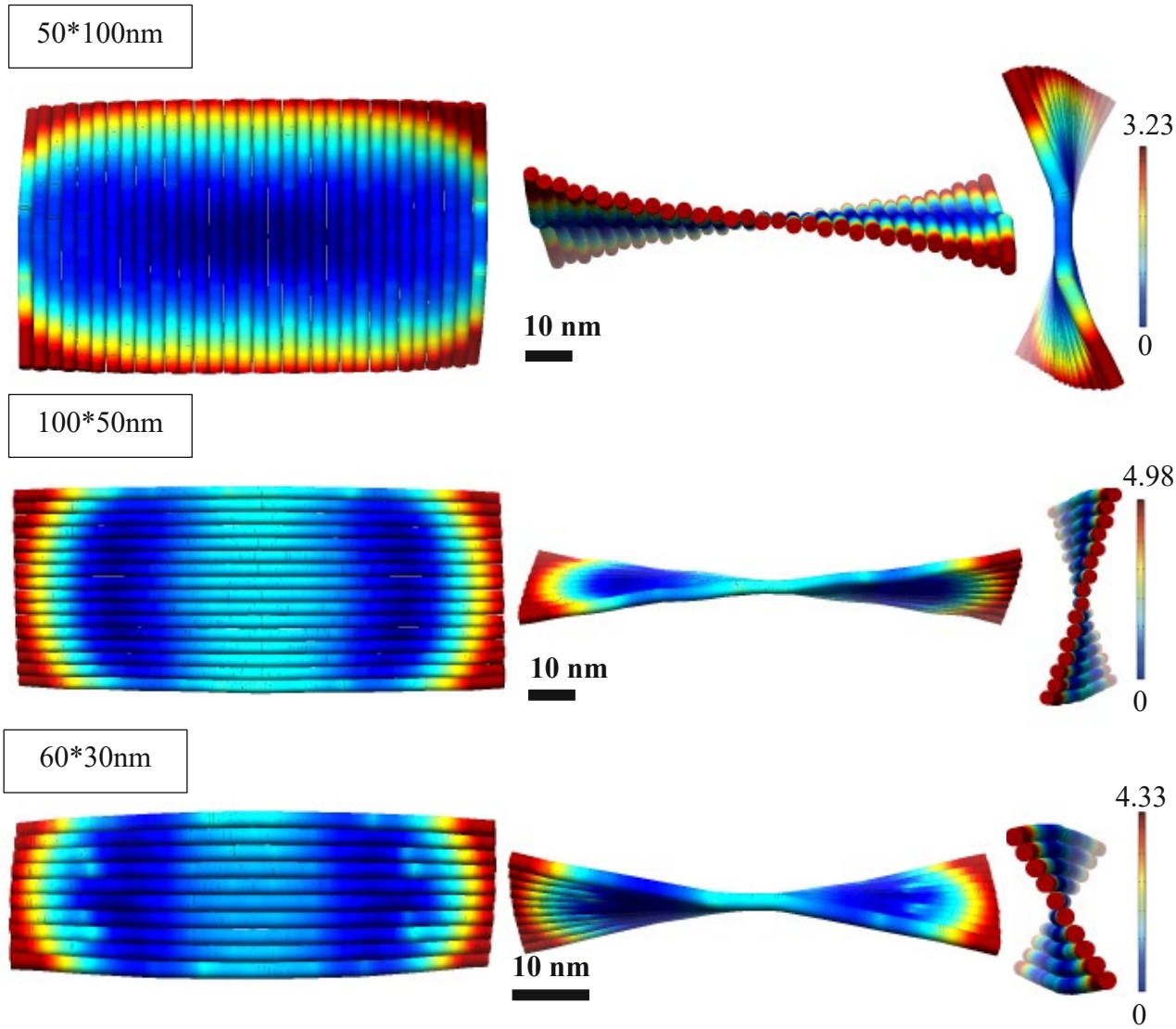


***Figure 20 CanDo root mean square fluctuation profiles***

*This figure shows different views of the root mean square fluctuation profiles of the three computationally designed platform version 50x100nm, 100x50nm and 60x30nm. Dark blue indicates the lowest fluctuation up to dark red which indicates the highest RMSF.*



Die approbierte gedruckte Originalversion dieser Diplomarbeit ist an der TU Wien Bibliothek verfügbar
The approved original version of this thesis is available in print at TU Wien Bibliothek.
TU Bibliothek Your knowledge hub WIEN

I further continued my experiments using the 50*100nm platform as it showed the lowest values of RMSF and therefore theoretically has the highest incorporation efficiency of the three variants. In order to identify if a binding strand forms a secondary structure, NUPACK [57] was used. The aim was to find a sequence that mirrors its complimentary bases having the mirror axis in the center and that does not form secondary structures with itself and the predesigned elongations of the binding sites. Two of such sequences had to be designed - X, V -, one for the binding between the hairpin X' elongations and the other for the binding between the V' elongations. In the image below the elongations X (green) of two X' hairpins (blue) are shown.

*Figure 21 Principle of interaction between platforms*

*After incorporation of the interaction strands (blue), binding strands (green) are added for attachment between platforms. One part of the binding strand pairs with the last nine bases of the interaction strand and the last 16 bases of the binding strand bind to the first 16 bases of another binding strands which is also connected to a platform therefore attaching two platforms. Per binding strand two Ts are left unpaired for flexibility.*

## 4.2 Characterization of DNA origami rectangles

In the following subsection I will describe the results of the experiments done for the evaluation of DNA origami integrity and the binding to the lipid bilayer. Due to limited time I had to reduce the scope of the experiment and chose to continue working with version 1, as reference, and version 3 for the analysis of interaction site specific oligomerization of lipid bilayer bound rectangular scaffolded DNA origami platforms.



Die approbierte gedruckte Originalversion dieser Diplomarbeit ist an der TU Wien Bibliothek verfügbar
The approved original version of this thesis is available in print at TU Wien Bibliothek.
TU Bibliothek Your knowledge hub WIEN

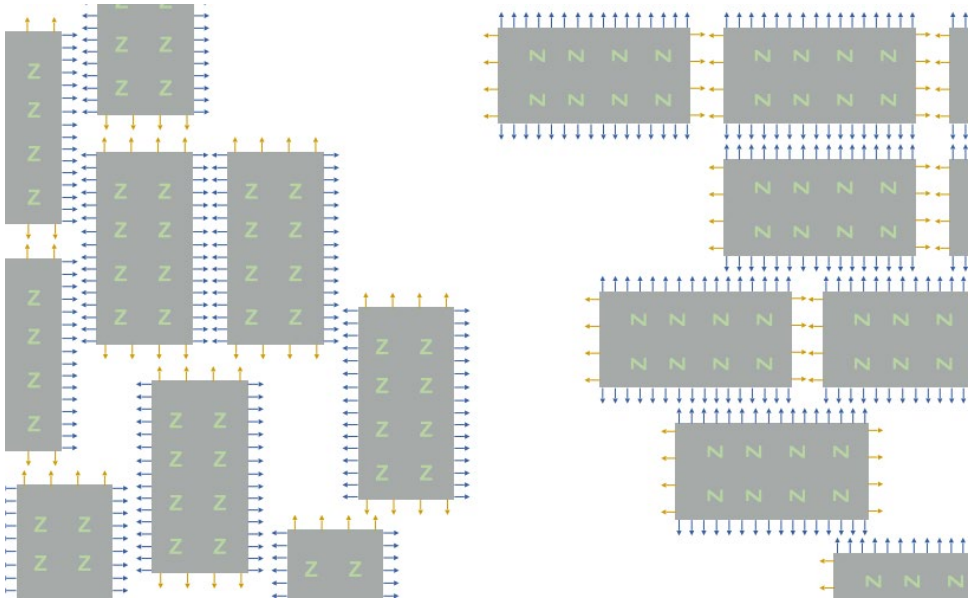

*Figure 22 Version 3: ways of binding*

*Visualization of the possible directionalities of version 3 DNA origami rectangles after self-assembly induced by addition of binding strands.*

### 4.2.1 Gel Electrophoresis

As control whether folding occurred and binding strands actually are able to crosslink platforms to larger aggregates in solution, gel electrophoresis was used. Gel electrophoresis separates DNA fragments in dependence of their size and was used to visualize the sizes of the formed DNA conglomerates. In figure 23 the gel is shown. In the first and last (eighth) well two different DNA ladders have been added, first the FastRuler™ Middle Range DNA Ladder (Thermo Scientific™) ranging from 100 to 5000 base pairs for rough quantification of double-stranded DNA and last the GeneRuler 1 kb DNA Ladder (Thermo Scientific™) ranging from 250 base pairs to 10,000 base pairs in order to assess the size of the formed DNA (origami) in the other wells. Between these ladders, samples of different variants of DNA have been placed. In the second well, the scaffold strand which consist of 7,249 nucleotides [3] was paced as a reference. Next the two versions, V1 and V3 have been inserted to control if the folding process was successful. In the following three wells, Version 3 has been placed with different combinations of added binding strands, first only the X binding strands which only allow for platform binding between the long sides of the rectangles, then only the V binding strands, only



Die approbierte gedruckte Originalversion dieser Diplomarbeit ist an der TU Wien Bibliothek verfügbar
The approved original version of this thesis is available in print at TU Wien Bibliothek.
TU Bibliothek Your knowledge hub WIEN

allowing interactions between the short sides of the platforms and last both X and V binding strands have been added combining the possible interactions described above. The addition of the binding strands to the Version 3 platforms was performed as mentioned in the section Material and Methods.

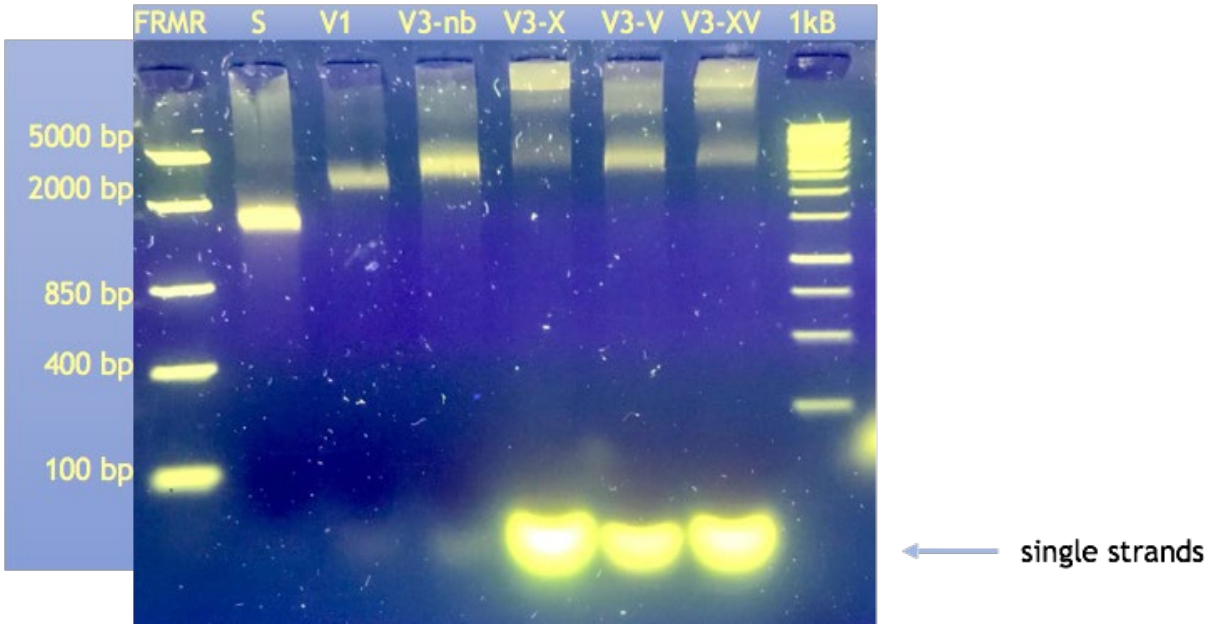


*Figure 23 Gel Electrophoresis*

*From from left to right: FRMR…Fast Ruler Middle Range DNA ladder; S…Scaffold Strand; V1…Version 1, Origami no binding sites; V3…Version 3, Origami binding sites - no binding strands added; V3-X…Version 3, Origami binding sites - X binding strands added; V3-V…Version 3, Origami binding sites - V binding strands added; V3-XV…Version 3, Origami binding sites - XV binding strands added; 1kB…1kB DNA ladder*

The gel shows that the number of base pairs, from which one can deduce the size of the folded platforms, is within the expected range of 4,000 to 5,000 bp.

What can be clearly seen analyzing the gel, is that when binding strands where added, especially binding strand X, oligomerization takes place in solution. Further, as expected, looking at column three and four, namely V1 and V3-nb (no binding strands added), the different versions of the DNA origami platform have approximately the same size and are roughly two times larger than the scaffold strand S found in the second column.

Die approbierte gedruckte Originalversion dieser Diplomarbeit ist an der TU Wien Bibliothek verfügbar
The approved original version of this thesis is available in print at TU Wien Bibliothek.
TU Bibliothek Your knowledge hub WIEN

### 4.2.2 Determination of yield

To measure the concentration of the two versions, V1 and V3, of the DNA origami platforms after spin column purification a spectrometer was used to measure the concentration of double stranded DNA via absorption at 260 and 280nm. The mean of the measured concentrations was ~15.5ng/µl for both V1 and V3.

| | | | |
|---|---|---|---|
| V1 | | | Spectrum |
| | 1.531 | 2.076 | 260/280 |
| | **16.75** | **14.158** | ng/µL |
| V3 | | | Spectrum |
| | 2.4 | 1.788 | 260/280 |
| | **14.417** | **16.615** | ng/µL |

*Table 4 Concentrations of DNA origami*

*Concentrations of dsDNA in Version 1 (V1) and Version 3 (V3) for two measurements each.*

### 4.2.3 AFM

Another way to visualize and characterize the DNA origami platforms is to use Atomic Force Microscopy. After several failed attempts of imaging the samples in air I switched to imaging the samples in buffer which looked a little more promising. By augmenting the driver amplitude, it was possible to elevate the relative setpoint. A high relative setpoint is needed so that the fragile sample under water is not harmed by the rapid movement of the cantilever. The smaller the window to be imaged is chosen the higher the line rate was chosen. Only at the very end of my experiments after using freshly ordered cantilevers some rectangles with the desired measurements could be visualized under the AFM in buffer *(Figure 24)*.

Die approbierte gedruckte Originalversion dieser Diplomarbeit ist an der TU Wien Bibliothek verfügbar
The approved original version of this thesis is available in print at TU Wien Bibliothek.
TU WIEN Bibliothek Your knowledge hub

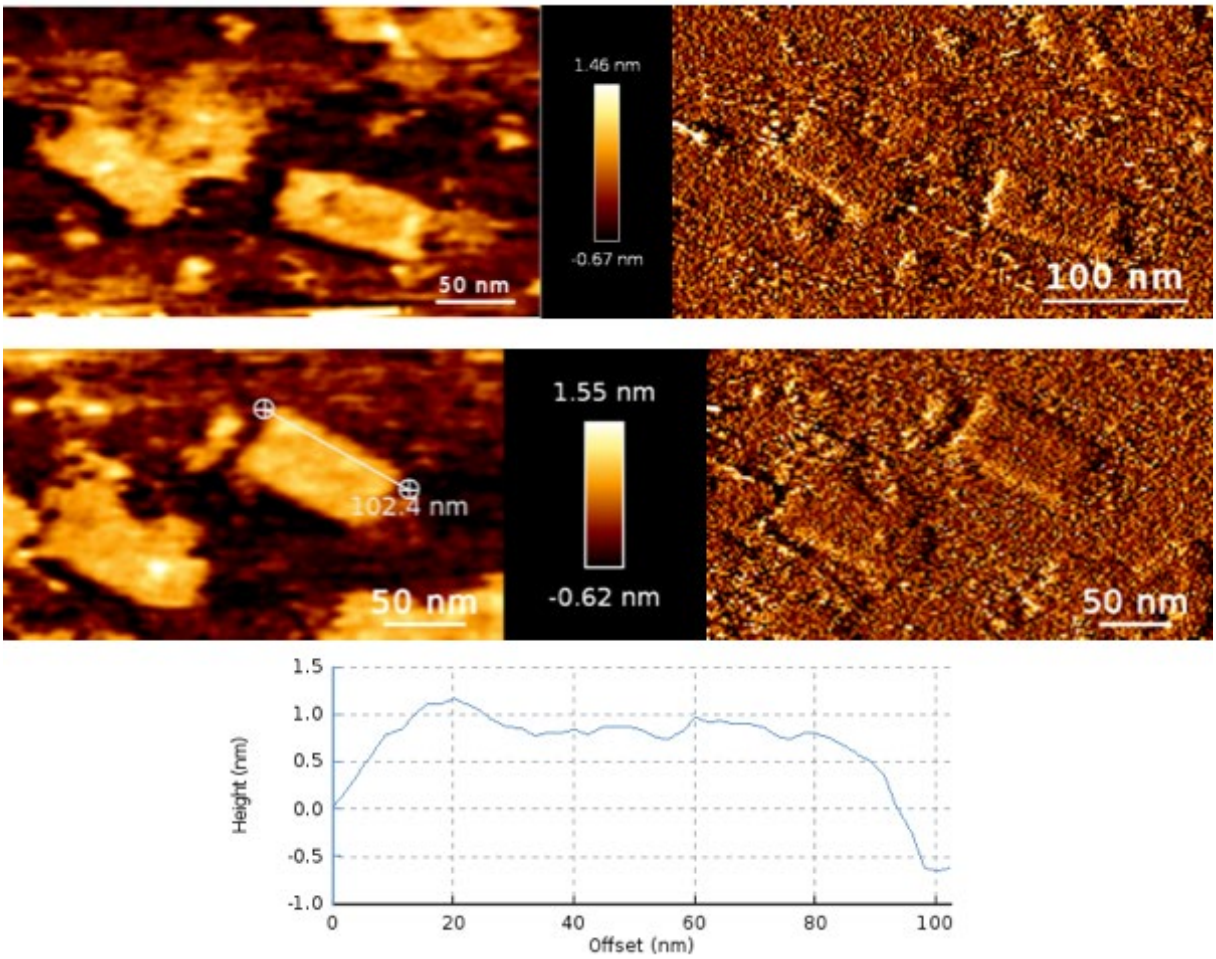


*Figure 24 AFM imaging of a DNA origami rectangle*

*In the top row and the second row an AFM image shows a correctly folded rectangular 100x50 DNA origami platform. The scalebar describes the height profile of the pictures. The third row shows the cross section indicated in the second row.*

As the clear formation of DNA origami rectangles could only be observed with AFM towards the end of the work done for this thesis and therefore the imaging of such was only possible twice, there is no clarity about the achieved yield of correctly folded DNA origami rectangles.

### 4.2.4 TIRF microscopy

In order to image the DNA origami and observe their oligomerization behavior, TIRF microscopy was used. Due to the labeling DNA origami with YOYO, for the visualization under the fluorescence microscope, the mixture undergoes spin column purification and the concentration of the sample decreases by half. 17µl of the YOYO stained DNA platforms



Die approbierte gedruckte Originalversion dieser Diplomarbeit ist an der TU Wien Bibliothek verfügbar
The approved original version of this thesis is available in print at TU Wien Bibliothek.
TU Bibliothek Your knowledge hub WIEN

(1.625 nM) were pipetted into a well of the Labtek chamber containing a SLB, visualized under blue laser light and recorded.

In order to verify that the DNA origami platforms are freely mobile on the SLB and determine whether V1 and V3 behave differently due to the additional interaction strands on the edges of V3 the mean squared displacement was calculated. Therefore, the MATLAB script, provided by members of the Institute of Applied Physics at TU Wien, first tracks the localizations and then calculates the trajectories of these bright YOYO stained DNA origami of the previously recorded images.

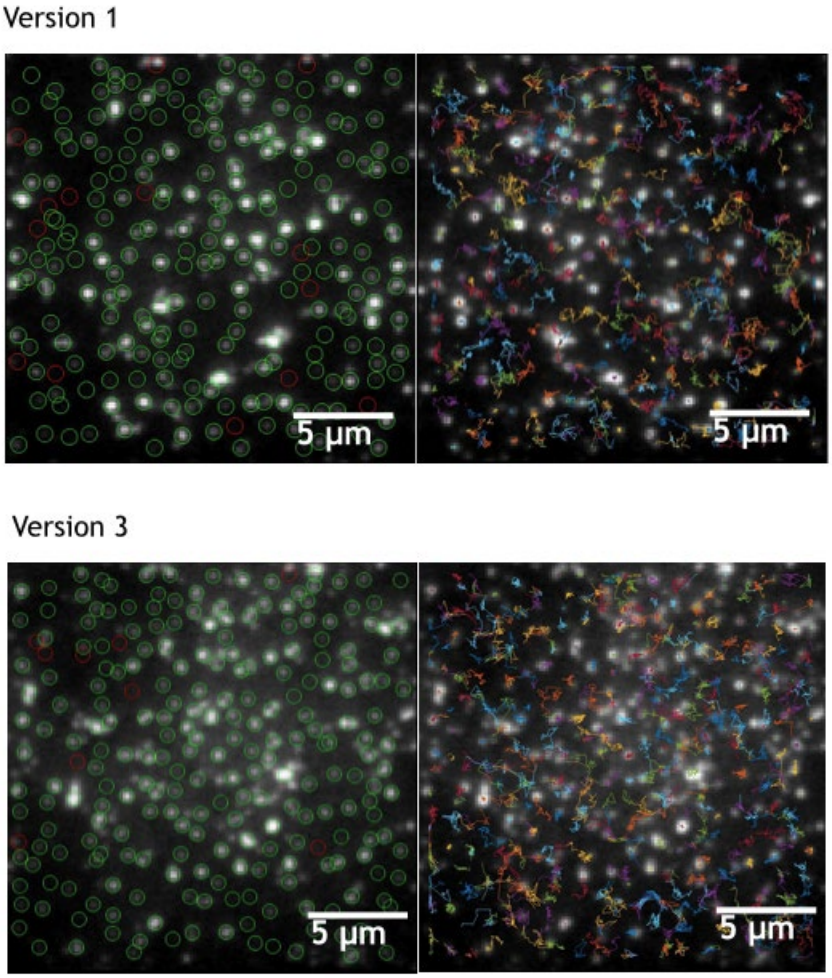


***Figure 25 Localization and tracking of DNA origami***

*The localization and the tracking of Version 1 (top) and Version 3 (bottom).*

The following figure shows the MSD plots calculated from representative frame sequences of version 1 and version 3.



Die approbierte gedruckte Originalversion dieser Diplomarbeit ist an der TU Wien Bibliothek verfügbar
The approved original version of this thesis is available in print at TU Wien Bibliothek.
TU Bibliothek Your knowledge hub WIEN

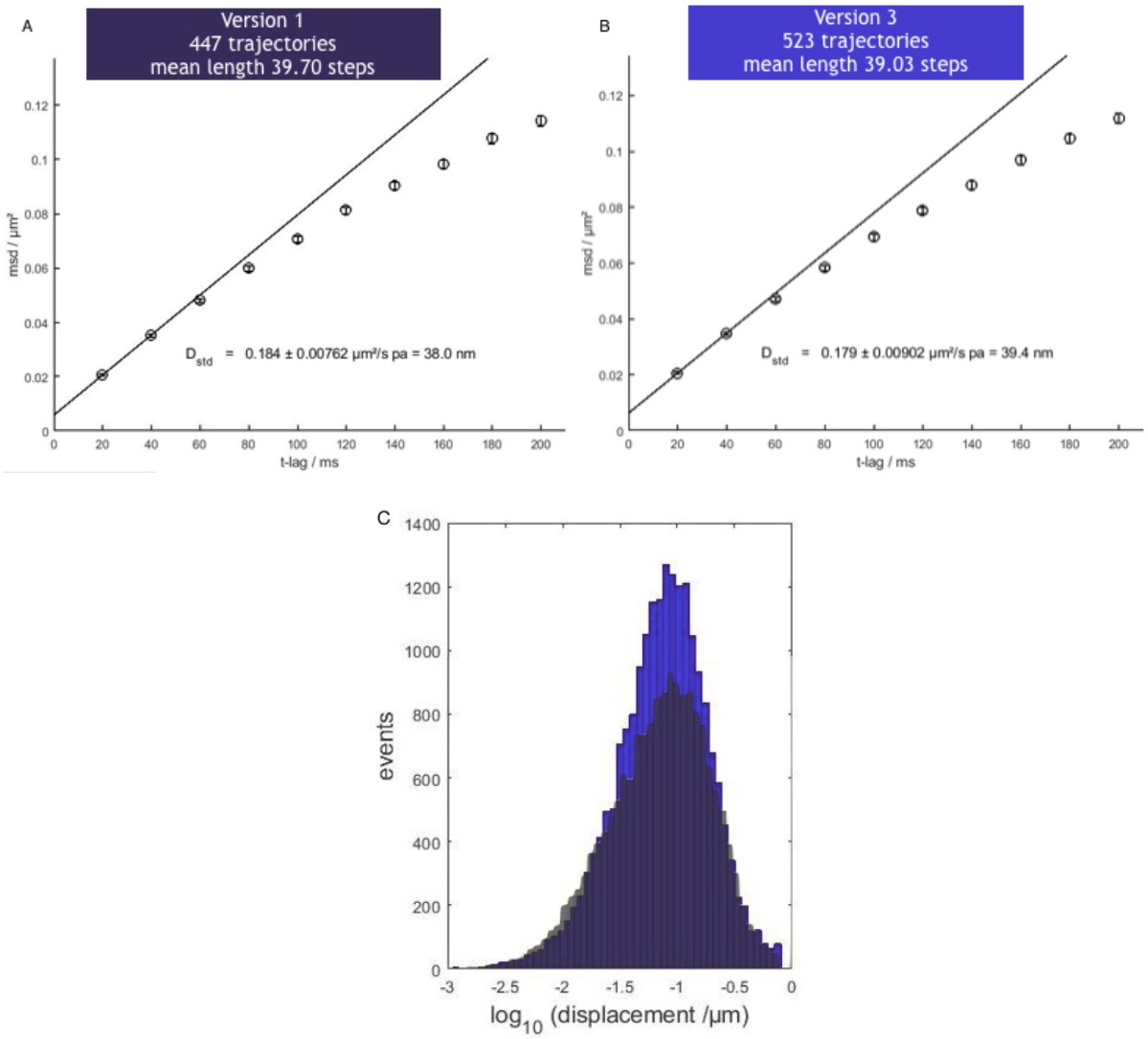


***Figure 26 Diffusion speed of DNA origami***

*A and B show the mean squared displacement per µm² plotted against the time lag per ms. The diffusion coefficient of version 1 is 0.184± 0.00762 µm²/s and of version 3 is 0.179± 0.00902 µm²/s. C shows the logarithmic displacement per µm plotted against the number of events of both versions 1 and 3 showing similar behavior.*

With D~0.18 µm²/s, the mobility seems to be low in comparison with other experiments [44] where the diffusion coefficient of approximately same sized DNA origami rectangles is around 0.25µm²/s with the same amount but differently placed cholesterol anchors. This suggests the presence of several immobile fluorescing particles, which were also observed under the microscope either being DNA origami platforms stuck in holes of the lipid bilayer or other unwanted particles that were fluorescently labeled in the process.



Die approbierte gedruckte Originalversion dieser Diplomarbeit ist an der TU Wien Bibliothek verfügbar
The approved original version of this thesis is available in print at TU Wien Bibliothek.
TU Bibliothek Your knowledge hub WIEN

In the first experiments the concentration of DNA origami platforms visualized under the microscope was not high enough to ensure binding between the platforms, as they have to be relatively near to each other to be able to interact. Therefore, the original staining protocol was changed in the way that a higher concentration of DNA origami platforms was used and one step in the centrifuge was eliminated (*see Methods*). Finally, after changing the protocol and practicing the production of DNA origami platforms I was able to obtain a concentration high enough to enable the binding of the DNA origami rectangles.

After addition of 5µl of 50 mM X and 50 mM V binding strands to 15.5ng/µl of version 3, and incubating the sample for 30 minutes at 37°C before the sample was stored in the fridge at 4°C for 24 h.

The aggregation of DNA origami platforms was observed by using TIRF microscopy. In *Figure 25* the formation of clusters about 100-fold the platform size are shown.

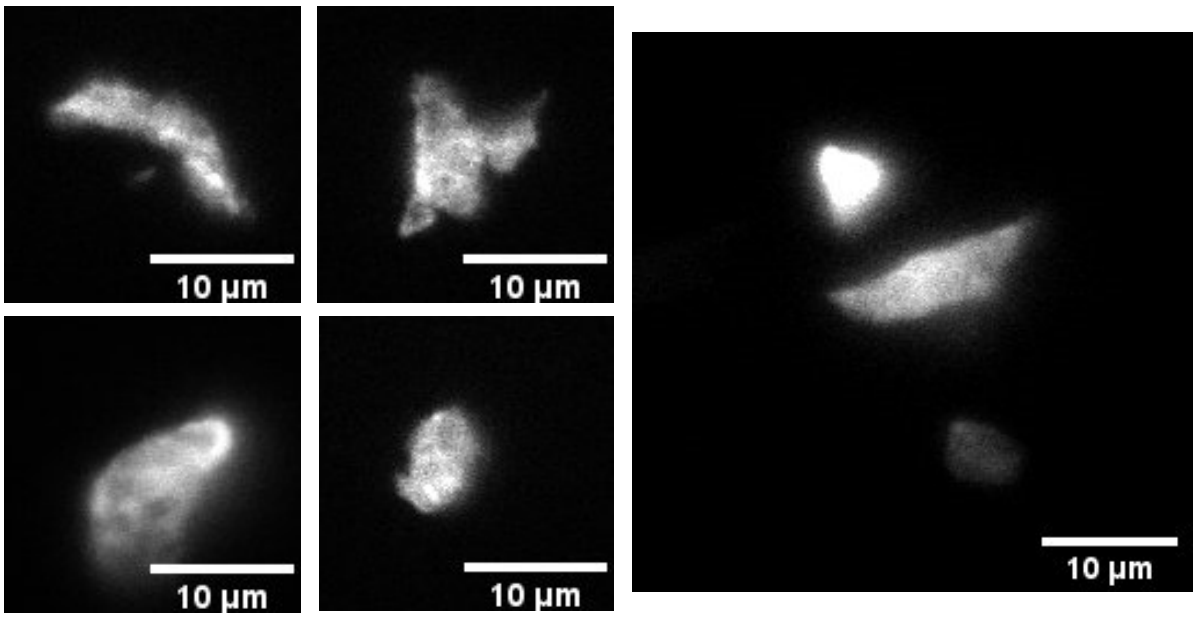


***Figure 27 Different formed aggregates***

*Resulting aggregation of V3 on a SLB, one day after the addition of binding strand observed with TIRF microscopy.*

After the incubation of the interaction strands bound to the hairpin like structures of the long edges of the platforms and the addition of binding strands to the folded DNA origami platforms clear formation of aggregates occurred and could be observed by using fluorescence



Die approbierte gedruckte Originalversion dieser Diplomarbeit ist an der TU Wien Bibliothek verfügbar
The approved original version of this thesis is available in print at TU Wien Bibliothek.
TU Bibliothek Your knowledge hub WIEN

microscopy. Most of the aggregates were fully or partly attached to the lipid bilayer, but fully detached conglomerates could be observed as well.

When observed under the fluorescence microscope the sizes and shapes of the formed aggregates differed and therefore no aggregation pattern can be deduced. A reason for very large conglomeration could be the excessive number of interaction sites, 16 per long edge of a rectangle, which could increase the probability of random and unwanted stacking between the platforms. Apart from the aggregates bound to the lipid bilayer, few large fluorescent platforms floating above the imaging plane as well as from the lipid bilayer partly detached aggregates were observed. Fully or partly detachment may occur due to high stress within the aggregated formation and different directional diffusion forces acting on the system as well as due to holes in the lipid bilayer that may develop after time.

The formation of oligomers also occurred in an Eppendorf tube which could be shown by using gel electrophoresis as analytical method.

Die approbierte gedruckte Originalversion dieser Diplomarbeit ist an der TU Wien Bibliothek verfügbar
The approved original version of this thesis is available in print at TU Wien Bibliothek.
TU WIEN Bibliothek Your knowledge hub

# 5 Conclusion and Outlook

In this thesis, I designed a DNA origami platform for surface-assisted self-assembly. The assembly process can be initiated in two axes on demand by adding binding strands. The design is versatile as the location and number of binding strands can be adjusted. For the verification of correct folding, AFM imaging was used. As the structures are very small and fragile, a high-speed atomic force microscope for imaging my produce better results. The higher scanning speed might minimize the allover systemic drift and would allow for several consecutive scans of the same area for image processing in order to reduce noise. Aggregation on SLB worked, but not only in 2D as wanted. In accordance, aggregation by addition of binding strands in solution was induced. I would recommend to reduce the number of interaction strands for the binding between platforms on the long edges to a minimum.

Further, increasing the number of cholesterol-modified DNA strands for better anchorage to the SBL could reduce the possibility of detachment of oligomerized platforms. Alternatively, one may use other ways to bind DNA origami to a lipid bilayer, for example by using electrostatic attraction forces or other methods [61]. The possibility of using mica instead of a lipid bilayer could be examined, where surface adhesion can be adjusted via the addition of $Mg^{2+}$ [19].

Die approbierte gedruckte Originalversion dieser Diplomarbeit ist an der TU Wien Bibliothek verfügbar
The approved original version of this thesis is available in print at TU Wien Bibliothek.
TU WIEN Bibliothek Your knowledge hub

# 6 Appendix

## 6.1 Abbreviations

| | |
|---|---|
| A | adenine |
| AFM | atomic force microscopy |
| C | cytosine |
| DNA | deoxyribonucleic acid |
| ds DNA | double stranded deoxyribonucleic acid |
| EDTA | ethylenediaminetetraacetic acid |
| FoB | folding buffer |
| G | guanine |
| $MgCl_2$ | magnesium chloride |
| MSD | mean squared displacement |
| NaCl | natrium chloride |
| NA | numerical aperture |
| PBS | phosphate-buffered saline |
| PCR | polymerase chain reaction |
| POPC | 1-palmitoyl-2-oleoyl-sn-glycero-3-phosphocholine |
| RMSF | root mean square fluctuation |
| RNA | ribonucleic acid |
| SDS | sodium dodecyl sulfate |
| SLB | supported lipid bilayer |
| T | thymine |
| TE | Tris-EDTA |
| TAE | Tris-acetate-EDTA |
| TIRF | total internal reflection fluorescence |
| Tris | tris(hydroxymethyl)aminomethane |
| up $H_2O$ | ultrapure water |
| UV | ultra violet |

Die approbierte gedruckte Originalversion dieser Diplomarbeit ist an der TU Wien Bibliothek verfügbar
The approved original version of this thesis is available in print at TU Wien Bibliothek.
TU Bibliothek Your knowledge hub WIEN

## 6.2 List of sequences

Mastermix 1: Staple Strands

| Name/Start | End | Sequence | Length |
|---|---|---|---|
| 11[208] | 9[207] | AACGTCACGGCGACATTCAACCGCGCCAAA | 30 |
| 15[272] | 13[271] | GGCTATCAGAATCGATGAACGGTTAAACGT | 30 |
| 21[160] | 23[159] | GCCCAATAATCTAAAGTTTTGTCGATGGGATT | 32 |
| 2[255] | 4[256] | GTTGCAGCTTGCGTATTGGGCGCCTCACTGCC | 32 |
| 8[175] | 5[175] | AAAATACACCGAGGAAACGCAAATGAAATAGCAATAGAGAGGGT | 44 |
| 25[272] | 23[271] | CGAGAATGCTATTATAGTCAGAACAAACTC | 30 |
| 7[160] | 9[159] | AGAAGGAAATACATAAAGGTGGCATAAGTTTA | 32 |
| 23[272] | 21[271] | CAACAGGTTGATAAGAGGTCATTTCCATAT | 30 |
| 3[160] | 5[159] | TGCCAGTTGAATAACATAAAAACACACCCTGA | 32 |
| 27[208] | 25[207] | TGAGGAAGGCCCACGCATAACCGATGACAA | 30 |
| 11[272] | 9[271] | GGAACAAATGGTGTAGATGGGCGTGCCGGA | 30 |
| 26[191] | 28[192] | GGTCGCTGTTTGAGGACTAAAGACTAAAATAC | 32 |
| 27[160] | 29[159] | AGGGTAGCACCTAAAACGAAAGAGCCCCCAGC | 32 |
| 0[231] | 1[223] | GAAAAACCGTCTATCAGAAAATCC | 24 |
| 10[191] | 12[192] | AGGGAAGGCCATTACCATTAGCAATAGCAGCA | 32 |
| 4[191] | 6[192] | GAAAATAGGCTAATATCAGAGAGAATAAGAGC | 32 |
| 3[208] | 1[207] | AAGAAACGGGTTTTGAAGCCTTATCCCGAC | 30 |
| 1[160] | 3[159] | TATCCGGTTACAATTTTATCCTGAGCCTAATT | 32 |
| 18[191] | 20[192] | CTATTATTAGAGGGTTGATATAAGCAGGAGGT | 32 |
| 25[208] | 23[207] | CAACCATCAAGGAATTGCGAATAAGAAAGG | 30 |
| 5[272] | 3[271] | GTGTAAAGTTAATTGCGTTGCGCAGGGTGG | 30 |
| 27[224] | 29[223] | TACGAGGCCAGATACATAACGCCAGATTTTAA | 32 |
| 13[208] | 11[207] | ACCAGAGCCAATGAAACCATCGAGGCCGGA | 30 |
| 18[247] | 16[240] | TTGTACCAAAAACATTTTATTTCAACGCAATCAAATCA | 38 |
| 0[167] | 1[159] | TTCATCGTAGGAATCAAGAAGGCT | 24 |
| 27[272] | 25[271] | ACGACGATGAAGTTTTGCCAGAGCAGAAAA | 30 |
| 13[272] | 11[271] | TAATATTTAGCTCATTTTTTAACCTCCGTG | 30 |
| 6[255] | 8[256] | GAGCTCGAGGTTTTCCCAGTCACGCGGTGCGG | 32 |
| 5[160] | 7[159] | ACAAAGTCCTATCTTACCGAAGCCAAGTTACC | 32 |
| 8[255] | 10[256] | GCCTCTTCCCGGCACCGCTTCTGGCATCGTAA | 32 |
| 19[160] | 21[159] | TACCAGGCGCCACCCTCAGAACCGGATAGCAA | 32 |
| 29[272] | 27[271] | GTTAATAAGAAAGATTCATCAGTTTACCAG | 30 |
| 10[255] | 12[256] | CCGTGCATAACAACCCGTCGGATTCAATAGGA | 32 |
| 7[208] | 5[207] | CTGGCATGGAGTTAAGCCCAATATAACCCA | 30 |
| 11[224] | 13[223] | ATCAACATCTGGCCTTCCTGTAGCGAAAAGCC | 32 |
| 24[175] | 21[175] | CCAAAAACAACTTTCAACAGTTATAGTTAGCGTAACGGGAACCC | 44 |
| 9[272] | 7[271] | AACCAGGCGTTGGGAAGGGCGATACGTTGT | 30 |
| 22[255] | 24[256] | TGGCTTAGCGAACCAGACCGGAAGGCAAAGCG | 32 |
| 23[160] | 25[159] | TTGCTAAAAAAGGCTCCAAAAGGATCGAGGTG | 32 |
| 17[208] | 15[207] | AACAGTTACAAATAAATCCTCATCTTGATA | 30 |
| 17[224] | 19[223] | GAGAAGCCTATGACCCTGTAATACGCGAGCTG | 32 |
| 26[247] | 24[240] | GTTTAGACTGGATAGATTGAATCCCCCTCACAAAAAGA | 38 |

Die approbierte gedruckte Originalversion dieser Diplomarbeit ist an der TU Wien Bibliothek verfügbar
The approved original version of this thesis is available in print at TU Wien Bibliothek.
TU WIEN Bibliothek Your knowledge hub

| | | | |
|---|---|---|---|
| 31[261] | 29[271] | AGCTGCTCATTCAGTGAAAGTAGTAAATTGGGCAATCTAC | 40 |
| 17[272] | 15[271] | ATATATTTGATTCAAAAGGGTGACTACAAA | 30 |
| 21[224] | 23[223] | TTAAATATTATAATGCTGTAGCTCCAAATATC | 32 |
| 28[255] | 30[256] | AGGAATACGGACGTTGGGAAGAAATTGAGATG | 32 |
| 31[228] | 29[239] | CCGGATATTCATTACCCAATCAACTTTAATCATTTCATTAT | 41 |
| 10[183] | 8[176] | TAAATATTGACGGAACAATCAATAGAAAATAAACGTAG | 38 |
| 1[224] | 3[223] | TGTTTGATGTTTGCCCCAGCAGGCATGAATCG | 32 |
| 9[208] | 7[207] | GACAAAAGATTAAGACTCCTTATAAAAGAA | 30 |
| 16[191] | 18[192] | GAATGGAACCTTGAGTAACAGTGCTTCGGAAC | 32 |
| 24[191] | 26[192] | TTCACGTTGATAGTTGCGCCGACAATATATTC | 32 |

Mastermix 2: Staple Strands

| Name/Start | End | Sequence | Length |
|---|---|---|---|
| 7[224] | 9[223] | GCGATTAAGGCGAAAGGGGGATGTGCCTCAGG | 32 |
| 18[255] | 20[256] | TAAATCGGATAGTAGTAGCATTAATTTCGCAA | 32 |
| 29[208] | 27[207] | GCCTGATATTTCCATTAAACGGGTTTTTCA | 30 |
| 4[255] | 6[256] | CGCTTTCCAACATACGAGCCGGAACGGGTACC | 32 |
| 16[175] | 13[175] | CTCTGAAACAGGAGGTTGAGGCACCCTCAGAACCGCCTTAGCGT | 44 |
| 31[197] | 29[207] | GACCTTCATCAAGAGTAAAATTGTGTCGAAATCTATCATC | 40 |
| 19[224] | 21[223] | AAAAGGTGTATTTTCATTTGGGGCAACATGTT | 32 |
| 16[255] | 18[256] | GGAGACAGGGATAAAAATTTTTAGCATAAAGC | 32 |
| 19[208] | 17[207] | CGGAATAGATGCCCCCTGCCTATCCGTATA | 30 |
| 24[255] | 26[256] | GATTGCATAATGCTTTAAACAGTTGGGGTAAT | 32 |
| 0[199] | 2[192] | ACTCATCGAGAACAAGGGCGTTTTAGCGAACCAATCAAGA | 40 |
| 5[208] | 3[207] | CAAGAATTATTTTTTGTTTAACGTCCAAAT | 30 |
| 8[191] | 10[192] | ATGTTAGCTCATATGGTTTACCAGATTGAGGG | 32 |
| 12[255] | 14[256] | ACGCCATCGCAAATATTTAAATTGAATCGTAA | 32 |
| 10[247] | 8[240] | CTGCCAGTTTGAGGGACTCCAGCCAGCTTTGCTATTAC | 38 |
| 15[160] | 17[159] | CAGCATTGTTTACCGTTCCAGTAAGTACTGGT | 32 |
| 26[255] | 28[256] | AGTAAAATCTATCATAACCCTCGTTGAGATTT | 32 |
| 16[239] | 13[239] | CCATCAAATGCCGGAGAGGGTATGTCAATCATATGTAAGGAAGA | 44 |
| 9[224] | 11[223] | AAGATCGCGACGACGACAGTATCGCAGCTTTC | 32 |
| 23[224] | 25[223] | GCGTTTTAGAAGCCCGAAAGACTTATCGTCAT | 32 |
| 5[224] | 7[223] | GTTATCCGCATAGCTGTTTCCTGTGCTGCAAG | 32 |
| 26[183] | 24[176] | AGGCTTGCAGGGAGTAAACAGCTTGATACCGAAAATCT | 38 |
| 20[191] | 22[192] | TTAGTACCTAACACTGAGTTTCGTTCCACAGA | 32 |
| 31[164] | 29[175] | AACGGTGTACAGACCAGGCTTACTTAGCCGGAACCAAGCGC | 41 |
| 23[208] | 21[207] | AACAACTACAACGCCTGTAGCATCACCAGT | 30 |
| 24[239] | 21[239] | TTAAGAGATTCGAGCTTCAAAGAGCTTAATTGCTGAAGCAACTA | 44 |
| 13[224] | 15[223] | CCAAAAACCCCCGGTTGATAATCATCTAGCTG | 32 |
| 6[191] | 8[192] | AAGAAACATAATAACGGAATACCCTACGCAGT | 32 |
| 15[208] | 13[207] | TTCACAAACACCACCGGAACCGCCACCGGA | 30 |
| 2[191] | 4[192] | TTAGTTGCATATTATTTATCCCAATCAAAAAT | 32 |
| 7[272] | 5[271] | AAAACGACACTCTAGAGGATCCCGCATAAA | 30 |
| 21[272] | 19[271] | AACAGTTGTGACCATTAGATACACATCCAA | 30 |
| 22[191] | 24[192] | CAGCCCTCTCAGCGGAGTGAGAATATAATTTT | 32 |
| 11[160] | 13[159] | AGCCAGCAAAGTTTGCCTTTAGCGGGTCATAG | 32 |



Die approbierte gedruckte Originalversion dieser Diplomarbeit ist an der TU Wien Bibliothek verfügbar
The approved original version of this thesis is available in print at TU Wien Bibliothek.
TU Bibliothek Your knowledge hub WIEN

| | | | |
|---|---|---|---|
| 0[263] | 2[256] | TTAAAGAACGTGGACTGGCAAAATCCCTTATACTGAGAGA | 40 |
| 9[160] | 11[159] | TTTTGTCAATTATTCATTAAAGGTGGAATTAG | 32 |
| 19[272] | 17[271] | TAAATCATAATAAAGCCTCAGAGAACCCTC | 30 |
| 15[224] | 17[223] | ATAAATTATATGATATTCAACCGTTTTTGCGG | 32 |
| 25[160] | 27[159] | AATTTCTTTAAAGGCCGCTTTTGCTCGGAACG | 32 |
| 8[239] | 5[239] | GCCAGCTGTTGGGTAACGCCAGATTCGTAATCATGGTCTCACAA | 44 |
| 20[255] | 22[256] | ATGGTCAATGTCTGGAAGTTTCATTTTGCGGA | 32 |
| 14[191] | 16[192] | GAGCCGCCAGGTCAGACGATTGGCTAAAGCCA | 32 |
| 14[255] | 16[256] | AACTAGCAGCTATTTTTGAGAGATGAAAGGCC | 32 |
| 17[160] | 19[159] | AATAAGTTATTAAGAGGCTGAGACTTGCTCAG | 32 |
| 28[191] | 30[192] | GTAATGCCGTACAACGGAGATTTGCGCGACCT | 32 |
| 18[183] | 16[176] | CTGAAACATGAAAGTTTAACGGGGTCAGTGAGCGCAGT | 38 |
| 13[160] | 15[159] | CCCCCTTAACCCTCAGAGCCACCAGCCGCCGC | 32 |
| 21[208] | 19[207] | ACAAACTAGTGTATCACCGTACTTATAGCC | 30 |
| 3[272] | 1[271] | TTTTTCTTCTTCACCGCCTGGCCAATCAAA | 30 |
| 3[224] | 5[223] | GCCAACGCCGTGCCAGCTGCATTAGTGAAATT | 32 |
| 12[191] | 14[192] | CCGTAATCTTTTCATAATCAAAATCTCCCTCA | 32 |
| 25[224] | 27[223] | AAATATTCCGTCCAATACTGCGGAAAAGGAAT | 32 |

Possible interaction strands: non elongated staple strands

| Name/Start | End | Sequence | Length | Mix-ID |
|---|---|---|---|---|
| 5[240] | 3[247] | TTCCACACAGTCGGGAAACCTGTGCGGGGAGAGGCGGT | 38 | no_Z'-Mix |
| 5[176] | 3[183] | AATTGAGCCAGCCTTTACAGAGAACAAAATAAACAGCC | 38 | no_Z'-Mix |
| 29[176] | 27[183] | GAAACAAAACTACGAAGGCACCAAACGGCTACAGAGGC | 38 | no_Z'-Mix |
| 13[176] | 11[183] | TTGCCATCAGTAGCGACAGAATCAAATCACCAGTAGCA | 38 | no_Z'-Mix |
| 21[176] | 19[183] | ATGTACCGGCCACCCTCAGAACCGGATAAGTGCCGTCG | 38 | no_Z'-Mix |
| 13[240] | 11[247] | TTGTATAAAAAAATAATTCGCGTTAAATGTGAGCGAGT | 38 | no_Z'-Mix |
| 29[240] | 27[247] | ACCAGTCACACATTCAACTAATGATAGTAAGAGCAACA | 38 | no_Z'-Mix |
| 21[240] | 19[247] | AAGTACGGTAACCTGTTTAGCTAGCATCAATTCTACTA | 38 | no_Z'-Mix |
| 30[255] | 31[260] | GTTTAATTATCAACGTAACAA | 21 | no_X'_V'-Mix |
| 2[183] | 0[168] | TATTTTGCACCCAGCATTCTAAGAACGCGACAAGCCGTTTTTATT | 45 | no_X'_V'-Mix |
| 29[160] | 31[163] | GATTATACGAGGCGCAGACGGTCAAGAGGACAGATG | 36 | no_X'_V'-Mix |
| 29[224] | 31[227] | GAACTGGCGTGAATTACCTTATGCTCTTGACAAGAA | 36 | no_X'_V'-Mix |
| 30[191] | 31[196] | GCTCCATGGCATAGGCTGGCT | 21 | no_X'_V'-Mix |
| 1[208] | 0[200] | TTGCGGGATAAACCAAGTACCGC | 23 | no_X'_V'-Mix |
| 1[272] | 0[264] | AGAATAGCAACAAGAGTCCACTA | 23 | no_X'_V'-Mix |
| 2[247] | 0[232] | AAGCGGTCCACGCTGGGTGGTTCCGAAATCCCAACGTCAAAGGGC | 45 | no_X'_V'-Mix |

Possible interaction strands: elongated staple strands

- Z‘ strand elongation: TTTTAGAGTCCTAGCATATTTAGCC
- X’ strand elongation: TTTTGCCAAGATAGACAGAAG
- V’ strand elongation: TTTTGTGGAGTAGTGTCATGT

Die approbierte gedruckte Originalversion dieser Diplomarbeit ist an der TU Wien Bibliothek verfügbar
The approved original version of this thesis is available in print at TU Wien Bibliothek.
TU WIEN Bibliothek Your knowledge hub

| Name | End | Sequence | Length |
|---|---|---|---|
| 5[240]-Z' | 3[247] | TTCCACACAGTCGGGAAACCTGTGCGGGGAGAGGCGGTTTTTAGAGTCCTAGCATATTTAGCC | 63 |
| 5[176]-Z' | 3[183] | AATTGAGCCAGCCTTTACAGAGAACAAAATAAACAGCCTTTTAGAGTCCTAGCATATTTAGCC | 63 |
| 29[176]-Z' | 27[183] | GAAACAAAACTACGAAGGCACCAAACGGCTACAGAGGCTTTTAGAGTCCTAGCATATTTAGCC | 63 |
| 13[176]-Z' | 11[183] | TTGCCATCAGTAGCGACAGAATCAAATCACCAGTAGCATTTTAGAGTCCTAGCATATTTAGCC | 63 |
| 21[176]-Z' | 19[183] | ATGTACCGGCCACCCTCAGAACCGGATAAGTGCCGTCGTTTTAGAGTCCTAGCATATTTAGCC | 63 |
| 13[240]-Z' | 11[247] | TTGTATAAAAAAATAATTCGCGTTAAATGTGAGCGAGTTTTTAGAGTCCTAGCATATTTAGCC | 63 |
| 29[240]-Z' | 27[247] | ACCAGTCACACATTCAACTAATGATAGTAAGAGCAACATTTTAGAGTCCTAGCATATTTAGCC | 63 |
| 21[240]-Z' | 19[247] | AAGTACGGTAACCTGTTTAGCTAGCATCAATTCTACTATTTTAGAGTCCTAGCATATTTAGCC | 63 |
| 30[255]-X' | 31[260] | GTTTAATTATCAACGTAACAATTTTGCCAAGATAGACAGAAG | 42 |
| 2[183]-X' | 0[168] | TATTTTGCACCCAGCATTCTAAGAACGCGACAAGCCGTTTTTATTTTTTGCCAAGATAGACAGAAG | 66 |
| 29[160]-X' | 31[163] | GATTATACGAGGCGCAGACGGTCAAGAGGACAGATGTTTTGCCAAGATAGACAGAAG | 57 |
| 29[224]-X' | 31[227] | GAACTGGCGTGAATTACCTTATGCTCTTGACAAGAATTTTGCCAAGATAGACAGAAG | 57 |
| 30[191]-X' | 31[196] | GCTCCATGGCATAGGCTGGCTTTTTGCCAAGATAGACAGAAG | 42 |
| 1[208]-X' | 0[200] | TTGCGGGATAAACCAAGTACCGCTTTTGCCAAGATAGACAGAAG | 44 |
| 1[272]-X' | 0[264] | AGAATAGCAACAAGAGTCCACTATTTTGCCAAGATAGACAGAAG | 44 |
| 2[247]-X' | 0[232] | AAGCGGTCCACGCTGGGTGGTTCCGAAATCCCAACGTCAAAGGGCTTTTGCCAAGATAGACAGAAG | 66 |
| 30[255]-V' | 31[260] | GTTTAATTATCAACGTAACAATTTTGTGGAGTAGTGTCATGT | 42 |
| 2[183]-V' | 0[168] | TATTTTGCACCCAGCATTCTAAGAACGCGACAAGCCGTTTTTATTTTTTGTGGAGTAGTGTCATGT | 66 |
| 29[160]-V' | 31[163] | GATTATACGAGGCGCAGACGGTCAAGAGGACAGATGTTTTGTGGAGTAGTGTCATGT | 57 |
| 29[224]-V' | 31[227] | GAACTGGCGTGAATTACCTTATGCTCTTGACAAGAATTTTGTGGAGTAGTGTCATGT | 57 |
| 30[191]-V' | 31[196] | GCTCCATGGCATAGGCTGGCTTTTTGTGGAGTAGTGTCATGT | 42 |
| 1[208]-V' | 0[200] | TTGCGGGATAAACCAAGTACCGCTTTTGTGGAGTAGTGTCATGT | 44 |
| 1[272]-V' | 0[264] | AGAATAGCAACAAGAGTCCACTATTTTGTGGAGTAGTGTCATGT | 44 |
| 2[247]-V' | 0[232] | AAGCGGTCCACGCTGGGTGGTTCCGAAATCCCAACGTCAAAGGGCTTTTGTGGAGTAGTGTCATGT | 66 |

Hairpin-Loops elongations: X' long side elongation TTTTGCCAAGATAGACAGAAG

Left side

| Name/Start | End | Sequence | Length |
|---|---|---|---|
| 0[136]-X'_long_side | 0[151] | TTACCGCGCCCAATAGTTTTGCCAAGATAGACAGAAG | 41 |
| 2[136]-X'_long_side | 2[151] | ATCTTACCAACGCTAATTTTGCCAAGATAGACAGAAG | 37 |
| 4[136]-X'_long_side | 4[151] | GGGAAGCGCATTAGACTTTTGCCAAGATAGACAGAAG | 37 |
| 6[136]-X'_long_side | 6[151] | CTTTTTAAGAAAAGTATTTTGCCAAGATAGACAGAAG | 37 |
| 8[136]-X'_long_side | 8[151] | ACATATAAAAGAAACGTTTTGCCAAGATAGACAGAAG | 37 |
| 10[136]-X'_long_side | 10[151] | GAATTATCACCGTCACTTTTGCCAAGATAGACAGAAG | 37 |
| 12[136]-X'_long_side | 12[151] | TCAGACTGTAGCGCGTTTTTGCCAAGATAGACAGAAG | 37 |
| 14[136]-X'_long_side | 14[151] | CCCTCAGAGCCGCCACTTTTGCCAAGATAGACAGAAG | 37 |
| 16[136]-X'_long_side | 16[151] | GCGTCATACATGGCTTTTTTGCCAAGATAGACAGAAG | 37 |
| 18[136]-X'_long_side | 18[151] | TCCTCAAGAGAAGGATTTTTGCCAAGATAGACAGAAG | 37 |
| 20[136]-X'_long_side | 20[151] | CCACCCTCAGAGCCACTTTTGCCAAGATAGACAGAAG | 37 |
| 22[136]-X'_long_side | 22[151] | TCTTTCCAGACGTTAGTTTTGCCAAGATAGACAGAAG | 37 |
| 24[136]-X'_long_side | 24[151] | GCCTTTAATTGTATCGTTTTGCCAAGATAGACAGAAG | 37 |
| 26[136]-X'_long_side | 26[151] | GGGATCGTCACCCTCATTTTGCCAAGATAGACAGAAG | 37 |
| 28[136]-X'_long_side | 28[151] | GCAAAAGAATACACTATTTTGCCAAGATAGACAGAAG | 37 |
| 30[136]-X'_long_side | 30[151] | ATCATAAGGGAACCGATTTTGCCAAGATAGACAGAAG | 37 |



Die approbierte gedruckte Originalversion dieser Diplomarbeit ist an der TU Wien Bibliothek verfügbar
The approved original version of this thesis is available in print at TU Wien Bibliothek.
TU WIEN Bibliothek Your knowledge hub

Right side

| Name/Start | End | Sequence | Length |
|---|---|---|---|
| 1[295]-X'_long_side | 1[280] | CCGAGATAGGGTTGAGTTTTGCCAAGATAGACAGAAG | 37 |
| 3[295]-X'_long_side | 3[280] | TTCACCAGTGAGACGGTTTTGCCAAGATAGACAGAAG | 37 |
| 5[295]-X'_long_side | 5[280] | CCTGGGGTGCCTAATGTTTTGCCAAGATAGACAGAAG | 37 |
| 7[295]-X'_long_side | 7[280] | GGCCAGTGCCAAGCTTTTTTGCCAAGATAGACAGAAG | 37 |
| 9[295]-X'_long_side | 9[280] | AAAGCGCCATTCGCCATTTTGCCAAGATAGACAGAAG | 37 |
| 11[295]-X'_long_side | 11[280] | CGGCGGATTGACCGTATTTTGCCAAGATAGACAGAAG | 37 |
| 13[295]-X'_long_side | 13[280] | TGTTAAAATTCGCATTTTTTGCCAAGATAGACAGAAG | 37 |
| 15[295]-X'_long_side | 15[280] | GGTCATTGCCTGAGAGTTTTGCCAAGATAGACAGAAG | 37 |
| 17[295]-X'_long_side | 17[280] | TAAATGCAATGCCTGATTTTGCCAAGATAGACAGAAG | 37 |
| 19[295]-X'_long_side | 19[280] | ACAGGCAAGGCAAAGATTTTGCCAAGATAGACAGAAG | 37 |
| 21[295]-X'_long_side | 21[280] | ATTCCCAATTCTGCGATTTTGCCAAGATAGACAGAAG | 37 |
| 23[295]-X'_long_side | 23[280] | CAGGATTAGAGAGTACTTTTGCCAAGATAGACAGAAG | 37 |
| 25[295]-X'_long_side | 25[280] | ACCATAAATCAAAAATTTTTGCCAAGATAGACAGAAG | 37 |
| 27[295]-X'_long_side | 27[280] | AAAAACCAAAATAGCGTTTTGCCAAGATAGACAGAAG | 37 |
| 29[295]-X'_long_side | 29[280] | AACGAACTAACGGAACTTTTGCCAAGATAGACAGAAG | 37 |
| 31[295]-X'_long_side | 31[280] | TAAGGCTTGCCCTGACTTTTGCCAAGATAGACAGAAG | 37 |

Die approbierte gedruckte Originalversion dieser Diplomarbeit ist an der TU Wien Bibliothek verfügbar
The approved original version of this thesis is available in print at TU Wien Bibliothek.
TU Bibliothek Your knowledge hub WIEN

# List of Figures


Figure 1 Chemical Structure of the four Nucleotides ..... 2
Figure 2 Five representations of the DNA Double Helix ..... 3
Figure 3 DNA nanotechnology ..... 5
Figure 4 Schematic drawing of folded DNA origami structure ..... 7
Figure 5 Workflow DNA origami ..... 8
Figure 6 Lipid Bilayer formation ..... 12
Figure 7 Jablonski diagram and Stokes shift ..... 14
Figure 8 Microscope scheme of components ..... 15
Figure 9 Total internal reflective fluorescence microscopy ..... 16
Figure 10 Airy disc ..... 18
Figure 11 Single Particle Tracking ..... 20
Figure 12 Atomic Force Microscopy Setup ..... 21
Figure 13 Particle Types ..... 23
Figure 14 Simulation Roadmap ..... 24
Figure 15 Simulation Snapshots ..... 25
Figure 16 Six Versions of DNA origami structures with different placements of strands for interaction ..... 26
Figure 17 PCR temperature profile ..... 31
Figure 18 Finished caDNAno Designs ..... 39
Figure 19 vHelix visualization ..... 40
Figure 20 CanDo root mean square fluctuation profiles ..... 41
Figure 21 Principle of interaction between platforms ..... 42
Figure 22 Version 3: ways of binding ..... 43
Figure 23 Gel Electrophoresis ..... 44
Figure 24 AFM imaging of a DNA origami rectangle ..... 46
Figure 25 Localization and tracking of DNA origami ..... 47
Figure 26 Diffusion speed of DNA origami ..... 48
Figure 27 Different formed aggregates ..... 49



Die approbierte gedruckte Originalversion dieser Diplomarbeit ist an der TU Wien Bibliothek verfügbar
The approved original version of this thesis is available in print at TU Wien Bibliothek.
TU Bibliothek Your knowledge hub WIEN

# List of Tables

TABLE 1 DNA ORIGAMI MIXES: 1 – 4 ..... 30
TABLE 2 DNA ORIGAMI MIXES: 5 & 6 ..... **ERROR! BOOKMARK NOT DEFINED.**
TABLE 3 LOADING PROBES FOR THE GEL ELECTROPHORESIS ..... 33
TABLE 4 RMSF FOR DIFFERENT DNA ORIGAMI PLATFORMS ..... 41
TABLE 5 CONCENTRATIONS OF DNA ORIGAMIS ..... 45

Die approbierte gedruckte Originalversion dieser Diplomarbeit ist an der TU Wien Bibliothek verfügbar
The approved original version of this thesis is available in print at TU Wien Bibliothek.
TU WIEN Bibliothek Your knowledge hub

# Bibliography


[1] N. C. Seeman, 'DNA in a material world', *Nature*, vol. 421, no. 6921, pp. 427–431, Jan. 2003, doi: 10.1038/nature01406.

[2] N. C. Seeman, 'Nucleic acid junctions and lattices', *Journal of Theoretical Biology*, vol. 99, no. 2, pp. 237–247, Nov. 1982, doi: 10.1016/0022-5193(82)90002-9.

[3] P. W. K. Rothemund, 'Folding DNA to create nanoscale shapes and patterns', vol. 440, p. 6, 2006.

[4] K. E. Dunn, 'The Business of DNA Nanotechnology: Commercialization of Origami and Other Technologies', *Molecules*, vol. 25, no. 2, p. 377, Jan. 2020, doi: 10.3390/molecules25020377.

[5] S. Li *et al.*, 'A DNA nanorobot functions as a cancer therapeutic in response to a molecular trigger in vivo', *Nat Biotechnol*, vol. 36, no. 3, pp. 258–264, Mar. 2018, doi: 10.1038/nbt.4071.

[6] V. Linko, A. Ora, and M. A. Kostiainen, 'DNA Nanostructures as Smart Drug-Delivery Vehicles and Molecular Devices', *Trends in Biotechnology*, vol. 33, no. 10, pp. 586–594, Oct. 2015, doi: 10.1016/j.tibtech.2015.08.001.

[7] N. C. Seeman, 'DNA nanotechnology', p. 23, 2017.

[8] P. Wang, T. A. Meyer, V. Pan, P. K. Dutta, and Y. Ke, 'The Beauty and Utility of DNA Origami', *Chem*, vol. 2, no. 3, pp. 359–382, Mar. 2017, doi: 10.1016/j.chempr.2017.02.009.

[9] C. Zhou, X. Duan, and N. Liu, 'A plasmonic nanorod that walks on DNA origami', *Nature Communications*, vol. 6, no. 1, Art. no. 1, Aug. 2015, doi: 10.1038/ncomms9102.

[10] D. Selnihhin, S. M. Sparvath, S. Preus, V. Birkedal, and E. S. Andersen, 'Multifluorophore DNA Origami Beacon as a Biosensing Platform', *ACS Nano*, vol. 12, no. 6, pp. 5699–5708, Jun. 2018, doi: 10.1021/acsnano.8b01510.

[11] B. Ding and N. C. Seeman, 'Operation of a DNA Robot Arm Inserted into a 2D DNA Crystalline Substrate', *Science*, vol. 314, no. 5805, pp. 1583–1585, Dec. 2006, doi: 10.1126/science.1131372.

[12] E. Kopperger, J. List, S. Madhira, F. Rothfischer, D. C. Lamb, and F. C. Simmel, 'A self-assembled nanoscale robotic arm controlled by electric fields', *Science*, vol. 359, no. 6373, pp. 296–301, Jan. 2018, doi: 10.1126/science.aao4284.




Die approbierte gedruckte Originalversion dieser Diplomarbeit ist an der TU Wien Bibliothek verfügbar
The approved original version of this thesis is available in print at TU Wien Bibliothek.
TU Bibliothek Your knowledge hub WIEN

[13] M. DeLuca, Z. Shi, C. E. Castro, and G. Arya, 'Dynamic DNA nanotechnology: toward functional nanoscale devices', *Nanoscale Horizons*, vol. 5, no. 2, pp. 182–201, 2020, doi: 10.1039/C9NH00529C.

[14] A. J. Griffiths, W. M. Gelbart, J. H. Miller, and R. C. Lewontin, 'The Nature of DNA', *Modern Genetic Analysis*, 1999, Accessed: Jul. 11, 2021. [Online]. Available: https://www.ncbi.nlm.nih.gov/books/NBK21261/

[15] B. Alberts, *Molecular biology of the cell*, Sixth edition. New York, NY: Garland Science, Taylor and Francis Group, 2015.

[16] C. T. Diagne, C. Brun, D. Gasparutto, X. Baillin, and R. Tiron, 'DNA Origami Mask for Sub-Ten-Nanometer Lithography', *ACS Nano*, vol. 10, no. 7, pp. 6458–6463, Jul. 2016, doi: 10.1021/acsnano.6b00413.

[17] R. A. Hughes and A. D. Ellington, 'Synthetic DNA Synthesis and Assembly: Putting the Synthetic in Synthetic Biology', *Cold Spring Harb Perspect Biol*, vol. 9, no. 1, p. a023812, Jan. 2017, doi: 10.1101/cshperspect.a023812.

[18] O. I. Wilner, Y. Weizmann, R. Gill, O. Lioubashevski, R. Freeman, and I. Willner, 'Enzyme cascades activated on topologically programmed DNA scaffolds', *Nature Nanotech*, vol. 4, no. 4, pp. 249–254, Apr. 2009, doi: 10.1038/nnano.2009.50.

[19] S. Woo and P. W. K. Rothemund, 'Self-assembly of two-dimensional DNA origami lattices using cation-controlled surface diffusion', *Nat Commun*, vol. 5, no. 1, p. 4889, Dec. 2014, doi: 10.1038/ncomms5889.

[20] J. Chen and N. C. Seeman, 'Synthesis from DNA of a molecule with the connectivity of a cube', *Nature*, vol. 350, no. 6319, pp. 631–633, Apr. 1991, doi: 10.1038/350631a0.

[21] E. Winfree, F. Liu, L. A. Wenzler, and N. C. Seeman, 'Design and self-assembly of two-dimensional DNA crystals', *Nature*, vol. 394, no. 6693, pp. 539–544, Aug. 1998, doi: 10.1038/28998.

[22] C. Mao, W. Sun, Z. Shen, and N. C. Seeman, 'A nanomechanical device based on the B–Z transition of DNA', *Nature*, vol. 397, no. 6715, pp. 144–146, Jan. 1999, doi: 10.1038/16437.

[23] D. Liu, M. Wang, Z. Deng, R. Walulu, and C. Mao, 'Tensegrity: Construction of Rigid DNA Triangles with Flexible Four-Arm DNA Junctions', *J. Am. Chem. Soc.*, vol. 126, no. 8, pp. 2324–2325, Mar. 2004, doi: 10.1021/ja031754r.

[24] W. B. Sherman and N. C. Seeman, 'A Precisely Controlled DNA Biped Walking



Die approbierte gedruckte Originalversion dieser Diplomarbeit ist an der TU Wien Bibliothek verfügbar
The approved original version of this thesis is available in print at TU Wien Bibliothek.
TU Bibliothek Your knowledge hub WIEN

Device', *Nano Lett.*, vol. 4, no. 7, pp. 1203–1207, Jul. 2004, doi: 10.1021/nl049527q.

[25] E. S. Andersen *et al.*, 'Self-assembly of a nanoscale DNA box with a controllable lid', *Nature*, vol. 459, no. 7243, pp. 73–76, May 2009, doi: 10.1038/nature07971.

[26] T. Omabegho, R. Sha, and N. C. Seeman, 'A Bipedal DNA Brownian Motor with Coordinated Legs', *Science*, vol. 324, no. 5923, pp. 67–71, Apr. 2009, doi: 10.1126/science.1170336.

[27] S. M. Douglas, I. Bachelet, and G. M. Church, 'A Logic-Gated Nanorobot for Targeted Transport of Molecular Payloads', *Science*, vol. 335, no. 6070, pp. 831–834, Feb. 2012, doi: 10.1126/science.1214081.

[28] B. Wei, M. Dai, and P. Yin, 'Complex shapes self-assembled from single-stranded DNA tiles', *Nature*, vol. 485, no. 7400, pp. 623–626, May 2012, doi: 10.1038/nature11075.

[29] Y. Suzuki, M. Endo, Y. Katsuda, K. Ou, K. Hidaka, and H. Sugiyama, 'DNA Origami Based Visualization System for Studying Site-Specific Recombination Events', *J. Am. Chem. Soc.*, vol. 136, no. 1, pp. 211–218, Jan. 2014, doi: 10.1021/ja408656y.

[30] S. Rinker, Y. Ke, Y. Liu, R. Chhabra, and H. Yan, 'Self-assembled DNA nanostructures for distance-dependent multivalent ligand–protein binding', *Nature Nanotech*, vol. 3, no. 7, pp. 418–422, Jul. 2008, doi: 10.1038/nnano.2008.164.

[31] H. Bila, E. E. Kurisinkal, and M. M. C. Bastings, 'Engineering a stable future for DNA-origami as a biomaterial', *Biomater. Sci.*, vol. 7, no. 2, pp. 532–541, 2019, doi: 10.1039/C8BM01249K.

[32] Y. He *et al.*, 'Hierarchical self-assembly of DNA into symmetric supramolecular polyhedra', *Nature*, vol. 452, no. 7184, pp. 198–201, Mar. 2008, doi: 10.1038/nature06597.

[33] J. List, M. Weber, and F. C. Simmel, 'Hydrophobic Actuation of a DNA Origami Bilayer Structure', *Angew. Chem. Int. Ed.*, vol. 53, no. 16, pp. 4236–4239, Apr. 2014, doi: 10.1002/anie.201310259.

[34] C. M. Erben, R. P. Goodman, and A. J. Turberfield, 'Single-Molecule Protein Encapsulation in a Rigid DNA Cage', *Angew. Chem. Int. Ed.*, vol. 45, no. 44, pp. 7414–7417, Nov. 2006, doi: 10.1002/anie.200603392.

[35] T. G. W. Edwardson, K. L. Lau, D. Bousmail, C. J. Serpell, and H. F. Sleiman, 'Transfer of molecular recognition information from DNA nanostructures to gold nanoparticles', *Nature Chem*, vol. 8, no. 2, pp. 162–170, Feb. 2016, doi: 10.1038/nchem.2420.

[36] S. M. Douglas, A. H. Marblestone, S. Teerapittayanon, A. Vazquez, G. M. Church, and



Die approbierte gedruckte Originalversion dieser Diplomarbeit ist an der TU Wien Bibliothek verfügbar
The approved original version of this thesis is available in print at TU Wien Bibliothek.
TU Bibliothek Your knowledge hub WIEN

W. M. Shih, ‘Rapid prototyping of 3D DNA-origami shapes with caDNAno’, p. 6, 2009.

[37] D.-N. Kim, F. Kilchherr, H. Dietz, and M. Bathe, ‘Quantitative prediction of 3D solution shape and flexibility of nucleic acid nanostructures’, *Nucleic Acids Research*, vol. 40, no. 7, pp. 2862–2868, Apr. 2012, doi: 10.1093/nar/gkr1173.

[38] C. E. Castro *et al.*, ‘A primer to scaffolded DNA origami’, *Nat Methods*, vol. 8, no. 3, pp. 221–229, Mar. 2011, doi: 10.1038/nmeth.1570.

[39] J.-P. J. Sobczak, T. G. Martin, T. Gerling, and H. Dietz, ‘Rapid Folding of DNA into Nanoscale Shapes at Constant Temperature’, *Science*, vol. 338, no. 6113, pp. 1458–1461, Dec. 2012, doi: 10.1126/science.1229919.

[40] V. Motsch, ‘Micro- and nanostructured surfaces for studying T cell activation’, p. 299.

[41] A. Aghebat Rafat, T. Pirzer, M. B. Scheible, A. Kostina, and F. C. Simmel, ‘Surface-Assisted Large-Scale Ordering of DNA Origami Tiles’, *Angewandte Chemie International Edition*, vol. 53, no. 29, pp. 7665–7668, 2014, doi: https://doi.org/10.1002/anie.201403965.

[42] S. Kocabey *et al.*, ‘Membrane-Assisted Growth of DNA Origami Nanostructure Arrays’, p. 10, 2015.

[43] C. A. Keller, K. Glasmästar, V. P. Zhdanov, and B. Kasemo, ‘Formation of Supported Membranes from Vesicles’, *Phys. Rev. Lett.*, vol. 84, no. 23, pp. 5443–5446, Jun. 2000, doi: 10.1103/PhysRevLett.84.5443.

[44] J. Hellmeier, ‘DNA Origami as a nanoscale tool for T cell activation’, p. 220.

[45] ‘Science of Fluorescence and Fluorescent Light Photography’. https://firedivegear.com/the-science-of-fluorescence/ (accessed Jul. 11, 2021).

[46] ‘File:Stokes shift.png - Wikipedia’. https://commons.wikimedia.org/wiki/File:Stokes_shift.png (accessed Jul. 11, 2021).

[47] ‘File:Jablonski Diagram of Fluorescence Only.png - Wikipedia’. https://commons.wikimedia.org/wiki/File:Jablonski_Diagram_of_Fluorescence_Only.png (accessed Jul. 11, 2021).

[48] ‘Figure 3. Optical basis of TIRF illumination. In epifluorescence...’, *ResearchGate*. https://www.researchgate.net/figure/Optical-basis-of-TIRF-illumination-In-epifluorescence-microscopy-the-excitation-light_fig3_51469494 (accessed Jul. 11, 2021).

[49] ‘File:Airy disk spacing near Rayleigh criterion.png - Wikipedia’. https://commons.wikimedia.org/wiki/File:Airy_disk_spacing_near_Rayleigh_criterion.png (accessed Jul. 11, 2021).

Die approbierte gedruckte Originalversion dieser Diplomarbeit ist an der TU Wien Bibliothek verfügbar
The approved original version of this thesis is available in print at TU Wien Bibliothek.
TU Bibliothek Your knowledge hub WIEN

[50] 'Figure 2.1: The Rayleigh criterion: Two points are regarded as just...', *ResearchGate*. https://www.researchgate.net/figure/The-Rayleigh-criterion-Two-points-are-regarded-as-just-resolved-when-the-principal_fig3_298070739 (accessed Jul. 11, 2021).

[51] M. F. Serag, M. Abadi, and S. Habuchi, 'Single-molecule diffusion and conformational dynamics by spatial integration of temporal fluctuations', *Nat Commun*, vol. 5, no. 1, p. 5123, Oct. 2014, doi: 10.1038/ncomms6123.

[52] C. Manzo and M. F. Garcia-Parajo, 'A review of progress in single particle tracking: from methods to biophysical insights', *Rep. Prog. Phys.*, vol. 78, no. 12, p. 124601, Dec. 2015, doi: 10.1088/0034-4885/78/12/124601.

[53] G. Binnig, C. F. Quate, and Ch. Gerber, 'Atomic Force Microscope', *Phys. Rev. Lett.*, vol. 56, no. 9, pp. 930–933, Mar. 1986, doi: 10.1103/PhysRevLett.56.930.

[54] 'Fig. 21 Working principle of an atomic force microscope (AFM)....', *ResearchGate*. https://www.researchgate.net/figure/Working-principle-of-an-atomic-force-microscope-AFM-Reproduced-with-permission-from_fig10_276924220 (accessed Jul. 11, 2021).

[55] C. Karner, C. Dellago, and E. Bianchi, 'Design of Patchy Rhombi: From Close-Packed Tilings to Open Lattices', *Nano Lett.*, vol. 19, no. 11, pp. 7806–7815, Nov. 2019, doi: 10.1021/acs.nanolett.9b02829.

[56] E. Benson *et al.*, 'DNA rendering of polyhedral meshes at the nanoscale', *Nature*, vol. 523, no. 7561, pp. 441–444, Jul. 2015, doi: 10.1038/nature14586.

[57] J. N. Zadeh *et al.*, 'NUPACK: Analysis and design of nucleic acid systems', *J. Comput. Chem.*, vol. 32, no. 1, pp. 170–173, Jan. 2011, doi: 10.1002/jcc.21596.

[58] J. J. Schmied *et al.*, 'DNA origami–based standards for quantitative fluorescence microscopy', *Nat Protoc*, vol. 9, no. 6, pp. 1367–1391, Jun. 2014, doi: 10.1038/nprot.2014.079.

[59] J. M. Majikes and J. A. Liddle, 'DNA Origami Design: A How-To Tutorial', *J. RES. NATL. INST. STAN.*, vol. 126, p. 126001, Jan. 2021, doi: 10.6028/jres.126.001.

[60] M. T. Strauss, 'Quantifying absolute addressability in DNA origami with molecular resolution', *NATURE COMMUNICATIONS*, p. 7, 2018.

[61] Q. Shen, M. W. Grome, Y. Yang, and C. Lin, 'Engineering Lipid Membranes with Programmable DNA Nanostructures', *Adv Biosyst*, vol. 4, no. 1, p. 1900215, Jan. 2020, doi: 10.1002/adbi.201900215.

Die approbierte gedruckte Originalversion dieser Diplomarbeit ist an der TU Wien Bibliothek verfügbar
The approved original version of this thesis is available in print at TU Wien Bibliothek.
TU Bibliothek Your knowledge hub WIEN